Effect of kaolin geopolymer ceramic on microstructure, thermal, spreadability and joint strength of Sn-3.0Ag-0.5Cu

N.S. Mohamad Zaimi[1, a], M. A. A. Mohd Salleh[1, b], M.M.A.B. Abdullah[1,c], R. Ahmad[2,d], S. Yoriya[3,e], J. Chaiprapa[4,f], G. Zhang[5,g] and D.M. Harvey[5,h]

[1]Center of Excellence Geopolymer & Green Technology (CeGeoGTech), School of Materials Engineering, Universiti Malaysia Perlis (UniMAP), Taman Muhibbah, 02600 Jejawi, Arau, Perlis, Malaysia
[2]Faculty of Engineering Technology, Uniciti Alam Campus, Universiti Malaysia Perlis (UniMAP), Perlis, Malaysia
[3]National Metal and Materials Technology Center, National Science and Technology Development Agency, 114 MTEC, Thailand Science Park, Pahonyothin Road, Khlong Neung, Khlong Luang, Pathum Thani 12120, Thailand
[4]Synchrotron Light Research Institute, Muang District, Nakhon Ratchasima 3000, Thailand
[5]General Engineering Research Institute, Liverpool John Moores University, Byrom Street, L3 3AF, United Kingdom

Email: [a]syahirahzaimi25@gmail.com, [b] arifanuar@unimap.edu.my, [c]mustafa_albakri@unimap.edu.my, [d]romisuhani@unimap.edu.my, [e]sorachy@mtec.or.th, [f]jitrin@slri.or.th, [g]G.Zhang@ljmu.ac.uk, [h]D.M.Harvey@ljmu.ac.uk

Keywords: Geopolymer ceramics, Composite solder, Intermetallics, Microstructure, Synchrotron Micro-XRF, Electron backscatter diffraction

Abstract

This paper investigates the effects of different weight percentage (0, 0.5, 1.0, 1.5 and 2.0 wt.%) of kaolin geopolymer ceramic (KGC) on the microstructure formations, thermal, spreadability and joint strength in Sn-3.0Ag-0.5Cu (SAC305) lead-free solder alloys in order to develop a new composite solder system. The composite solder was fabricated usingthe microwave sintering method and soldered on copper substrates. Advanced characterization techniques such as Electron backscatter diffraction (EBSD) and Synchrotron Micro-XRF were used to study the behaviors of the pure SAC305 and KGC reinforced SAC305 composite solders. Experimental results shows that the addition of KGC refines the β-Sn area and increases the eutectic area with fine intermetallics formation. The EBSD analysis shows that the crystal orientation of β-Sn in the KGC

reinforced SAC305 composite solder is changed to single orientation. In addition, the thickness of IMC layer is reduced with the reduction in the undercooling value for the KGC reinforced SAC305 composite solder. The spreadability of the KGC reinforced SAC305 composite solder is significantly increased in the spreadable area with a higher strength of solder joint. Besides that, the results obtained prove that 1.0 wt.% KGC addition gives better performances in terms of microstructure formations, thermal properties, spreadability and joint strength. Synchrotron Micro-XRF indicated that, some Al and Si, which are the major elements in geopolymer systems, are migrated into the solder area.

1.0 Introduction

The transition to lead free solder alloy has begun for more than a decade due to the prohibition in the consumption of lead in solder alloy by Restriction of Hazardous Substance (RoHS) and The Waste of Electrical and Electronic Equipment (WEEE) in the electronic packaging industries [1]. The elimination of lead in the solder alloy was due to the toxicity of lead which negatively influence the human and environments. Therefore, this triggered extensive researches to develop a ‘green’ solder alloy. Concurrently, the electronic packaging industry nowadays has grown very rapidly with development of advance electronics that demands for the usage of very reliable solder interconnections in the electronics products. A high reliable solder alloy is very crucial in electronics packaging since it will electrically and mechanically join the components and to ensure the overall functionality of the products. Thus, there exist many organizations such as Institute of Printed Circuits (IPC), The National Electronics Manufacturing Initiative (NEMI), the National Institute of Standard and Technology (NIST) and the National Center for Manufacturing Science (NCMS) that are actively searching for the best solder alloys in replacement of tin lead solder and implemented into the electronic products [2]. Among the various emerging lead free solder, Sn-Ag-Cu (SAC) lead free solder alloy posed the most outstanding choice by the industry in replacing conventional Sn-Pb solder alloy [2, 3]. This was owing to SAC lead free solder alloy shows a good wettability, better solder joint strength and lower melting point than the other Sn-based solder alloys [4-6]. However, still the performance of SAC could not meet or better than conventional lead solder especially on thermal cyclic condition [7]. On top of that, other major concerns

related with SAC are the formation of large and brittle intermetallic compounds (IMC) which can reduce the mechanical strength and solder reliability [6]. In typical SAC solder joint, the large and brittle IMC arise at higher undercooling of β-Sn (~10-40 K) which promotes the formation of large primary IMCs Cu_6Sn_5 rods and Ag_3Sn plates [8]. Since IMCs are brittle, controlling its growth is necessary in obtaining a strong solder joint.

Microelectronic technology develops rapidly with high demand in many applications for various fields. Currently, the microelectronic devices become more complicated with shrunk size, which bring the solder interconnections down to smaller sizes. Significant research works have been done in finding suitable and compatible solder alloys as to replace the conventional tin lead solder and also to fulfill the demands of high reliable solder alloys to be used in complex and future microelectronic devices. Recently, the emerging of composite solder technology attracted most of researchers worldwide. Introduction of reinforcing particles which are either metals or non-metals into the matrix of solder alloy by forming composite solder were likely to improve the performance and properties of existing solder alloys. Generally, reinforcing matrix of solder alloys with ceramic particles gain an interest among the researchers as a method to improve the existing solder alloy properties. This was due to the ceramic reinforcements were extremely stable at high temperature and no new excessive phase will form either during the fabrication or due to the large temperature difference between the reinforcing particles and solder alloys [2, 6]. Reinforcing the solder matrix with small amounts of ceramic particles including cerium oxide (CeO_2) [9, 10], zirconia (ZrO_2) [11, 12], titanium oxide (TiO_2) [2, 13-18], silicon carbide (SiC) [19, 20], silicon nitride (Si_3N_4) [21, 22], iron oxide (Fe_2O_3) [23], strontium titanate ($SrTiO_3$) [24], titanium carbide (TiC) [25], silicon dioxide (SiO_2) [26], lanthanum oxide (La_2O_3) [27] and aluminium oxide (Al_2O_3) [28, 29] have shown to improve microstructure formations, mechanical and thermal properties of solder. Li et al. [9] hypothesized that the incorporation of ceramic particles in solder matrix may act as heterogenous nucleation sites for β-Sn and eutectic phase which could increase the nucleation rate and may result in smaller grain size. Besides that, Gain et al. [12] has hypothesized that the shear strength of Sn-Ag-Cu was higher than the unreinforced solder even though it was subjected to multiple reflow cycles due to the homogenous distributions of ceramic particles that lead to dispersion strengthening

mechanism. It was also proved that ceramics particles could absorb in the molten solder during soldering process thereby limiting the substrate dissolution and diffusion which could in turns decrease the thickness of interfacial IMC layer and later beneficial to the strength of solder joints [30].

Geopolymer is an inorganic polymer material that formed through geopolymerization process involving the dissolution of aluminosilicate sources material which consist of SiO_2 and Al_2O_3 in highly alkaline activated solution producing amorphous to semi-crystalline structures with Si-O-Al and Si-O-Si bonds [31]. Interestingly, geopolymer powder can be used to produce geopolymer ceramics through sintering process yielding crystalline phases which required slightly low sintering temperature with excellent mechanical properties as compared to the typical ceramic [32-34]. This fabrication process was beneficial towards reducing the consumption of higher energy for the production of ceramics [35]. In addition, geopolymer ceramic consists of elements which may act as additional nucleation sites to improve the properties of solder alloys. Various hypothese were reported on the incorporation of ceramic particles to existing solder alloys. However, to the best of author knowledge, there is still no research being reported on the effect of using kaolin geopolymer ceramic as the reinforcement particles that may positively affect the existing solder alloys. Thus, this paper aims to investigate the effect of geopolymer ceramics as the potential reinforcement particles in Sn-Ag-Cu solder alloys which could improve the microstructure, thermal and mechanical properties of Sn-Ag-Cu solder alloys.

2.0 Experimental Procedure

2.1 Sample preparation

In this study, Sn-3.0Ag-0.5Cu (SAC305) solder powders with an average particle size in the range between 25 to 45 µm were used as the base matrix material. Kaolin geopolymer ceramics with an average particle size of <38 µm were used as reinforcement materials. Kaolin (supplied by Associated Kaolin Industries Sdn Bhd, Malaysia) were used as raw materials in the production of kaolin geopolymer ceramics. Then, kaolin was mixed with the alkaline activator solution and cured at temperature of 80 ˚C for 24 hours to form

kaolin geopolymer. The kaolin geopolymer were then crushed by using a mechanical crusher, compacted by using uniaxial pressing at a pressure of 4.5 tonnes and sintered at temperature of 1200 ˚C with 180 minutes of soaking time in order to form kaolin geopolymer ceramics. Then, the sintered kaolin geopolymer ceramics had undergo ball milling process in a planetary mill machine for 10 hours with a speed of 450 rpm and ball to powder ratio of 10:1, so as to produce kaolin geopolymer ceramic powders with the size of less than 38 µm. The morphology of SAC305 and kaolin geopolymer ceramics were shown in Figure 1, respectively. The chemical composition of kaolin geopolymer ceramics based on X-ray fluorescence spectroscopy (XRF) was tabulated in Table 1. The main chemical compositions of kaolin geopolymer ceramics were Na_2O, Al_2O_3, SiO_2, K_2O and Fe_2O_3.

The fabrication of SAC305/kaolin geopolymer ceramics composite solder were done by using powder metallurgy route. Various weight percentage (wt.%) of kaolin geopolymer ceramics (0, 0.5, 1.0, 1.5 and 2,0 wt.%) were homogeneously mixed in air tight container by using planetary mill at a speed of 200 rpm for an hour. The solder mixtures were uniaxially compacted in a 12 mm stainless steel mold by using a Specac-15 tonnes Manual Hydraulic Press. The cylindrical pellets were compacted by using a pressure of 4.5 tonnes. Then, the compacted pellets were sintered by using a hybrid microwave sintering technique at 185 ˚C under ambient conditions by using 800 W, 50 Hz Panasonic oven for 3 minutes. A microwave susceptor material of silicon carbide (SiC) was used in this study.

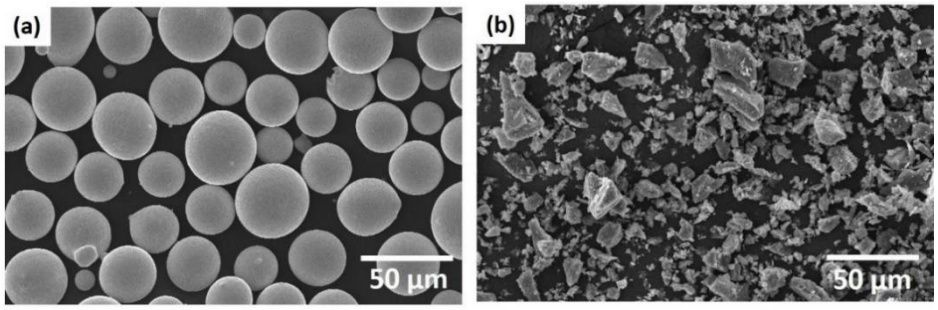

Figure 1: Morphology of (a) Sn-3.0Ag-0.5Cu and (b) Kaolin geopolymer ceramic

Table 1 : Chemical composition of kaolin geopolymer ceramic by XRF

Compound	Content (wt.%)
Na_2O	4.5
Al_2O_3	31.9
SiO_2	56.6
K_2O	2.50
TiO_2	0.74
MnO_2	0.05
Fe_2O_3	2.83
ZrO_2	0.05
LOI	0.83

2.2 Microstructure analysis

The microstructure of compacted sintered pellets was analyzed by using scanning electron microscope (SEM) in backscattered electron imaging mode in order to observe the distributions of kaolin geopolymer ceramics. The pellets were etched by using dilute solution of 2% hydrochloric acid (HCl), 5% nitric acid (HNO_3) and 93% methanol (CH_3OH) in order to have a clear grain boundary observation. In fabricating solder balls, compacted sintered pellets were rolled into thin sheets with the thickness of approximately 50 µm sheets. The thinned sheets were punched by using a 3.0 mm puncher in order to prepare a 900 µm diameter solder ball. The punch sheets were then dipped in rosin mildly activated flux (RMA) and melted on Pyrex plate at a temperature of 250 °C in a reflow oven. The solder balls with spherical shape were formed due to the action of surface tension during melting of solder sheets. Subsequently, the solder balls were sieved with the sieves of 1 mm and 0.9 mm in size in order to obtain uniform size of solder balls. In order to form solder joints, the fabricated solder balls were reflowed on a 900 µm ball pitch size of Cu substrate printed circuit board (PCB) with an organic soldering perspective (OSP) surface finish and a small amount of RMA flux was applied prior to reflow soldering process. The reflow soldering process was carried out by using a F4N desktop reflow oven. The reflowed samples were cross sectioned, cold-mounted in epoxy resin, grinded with SiC paper and polished. The microstructure of reflowed samples were analysed by using scanning electron microscope (SEM), electron backscattered

diffraction (EBSD) and Synchrotron Micro-XRF (μ-XRF).The morphology and thickness of interfacial intermetallic compound (IMC) layer of the solder joints were observed by using scanning electron microscope (SEM). The thickness of IMC layer was evaluated by using J-Image software. The measurements of IMC thickness (t) were calculated as the area of IMC (A) divided with the length of IMC (L).

Electron backscattered diffraction (EBSD) samples were firstly ion-milled by using Hitachi IM-4000 ion milling equipment for about 10 minutes with rotation speed of 25 rpm. Then, the regions of solder ball were covered by a conductive layer of carbon in order to eliminate the effects of charging. During the EBSD testing, the samples were tilted to 70° and Hitachi SU8230 scanning electron microscope equipped with Nordlys EBSD detector, operated at 25 kV was used. Besides that, during EBSD acquisition, a step size of 1.5 μm was used. The Emax Evolution software were used for the analysis.

In order to investigate the interactions of kaolin geopolymer ceramic (KGC) to Sn-3.0Ag-0.5Cu (SAC305) lead free solder, a small bar of bulk KGC (5 x 10 x 30 mm) was dipped in molten SAC solder at 250 ºC for approximately 10 minutes and subsequently was cooled in air. Then, the samples were carefully fine polishing before it was analysed under synchrotron micro-XRF (μ-XRF). The schematic diagram for the experimental setup was shown in Figure 2. To precisely analysed the interaction between KGC to SAC solder, a detail elemental distributions analysis using synchrotron micro-XRF was performed at Synchrotron Light Research Institute (SLRI) Thailand at beamline BL6b. By using synchrotron radiation and 30 x 30 μm^2 size of beam focused by the polycapillary lens, the element distributions in the solder was obtained. Samples were placed at a 90° level between the X-ray and the CCD camera. The Vortex EM-650 silicon drift detector was used to collect the emitted fluorescence X-Ray and the area of interest was accurately specified by using high precision motorized stages. A 0.05 mm scanning step with exposure time of 10 s for each point were used. The data obtained was then analysed by using PyMca software. The area of interest with the size of 750 μm X 700 μm of the sample were scanned during synchrotron micro-XRF testing.

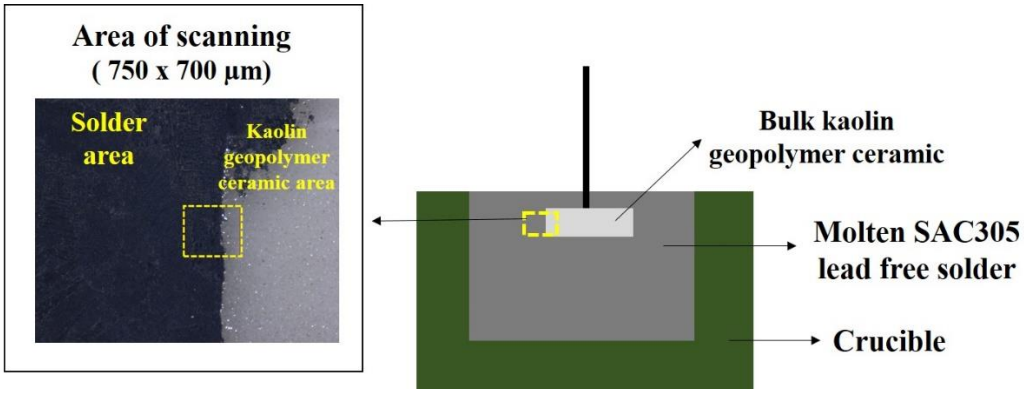

Figure 2 : Schematic diagram for the experimental setup dipping of bulk kaolin geopolymer ceramic in SAC305 lead free solder

Wetting behavior of all the samples were investigated by measuring a spreading area on copper (Cu) substrate. A Cu substrate of 30 mm x 30 mm x 0.3 mm was used in this study. The Cu substrate was finely polished and cleaned with the acid cleaning liquid which consists mixture of 5 g hydrochloric acid and 95 g deionized water to remove surface impurities on Cu substrates. Subsequently, 0.3 g of solder sheets were placed on Cu substrates with 0.03 g RMA flux. The samples were then reflowed in a F4N reflow oven and the spreading areas were measured by using J-Image software.

2.3Thermal properties analysis

The melting characteristics of all the samples were characterized by using a TA Instruments Differential Scanning Calorimetry (DSC). The samples used for DSC testing were as-rolled thin solder sheets. The weight for each of the samples were kept below 5 mg according to the requirement of DSC equipment and placed into an aluminum pan. All the samples were heated up to 250 °C and immediately cooled down to room temperature with a heating rate of 10 °C/min under a nitrogen gas (N_2) atmosphere. The thermal reactions for all the samples were determined based on the endothermic (heating) and exothermic (cooling) temperature curves.

2.4 Mechanical properties test

A single-lap shear solder joint test was performed in order to evaluate the strength of the solder joints which were bonded to the Cu substrate (PCB FR4-type). The single-lap shear test was conducted by using an Instron machine with the specifications of Cu substrate used as according to ASTM D1002 standard. According to the ASTM standard, the measurements of Cu substrate which is 101.6 mm x 25.4 mm x 1.5 mm (Figure 3) was used. Consistently about 1 g of solder sheets were sandwiched between Cu substrates. Reflow soldering process was performed in order to form a bonding between the Cu substrates with the aid of RMA flux, following the reflow profile proposed by Qualitek for lead free solder. Subsequently, the fracture analysis after the shear test was analyzed by using the scanning electron microscope at an accelerating voltage of 20 kV.

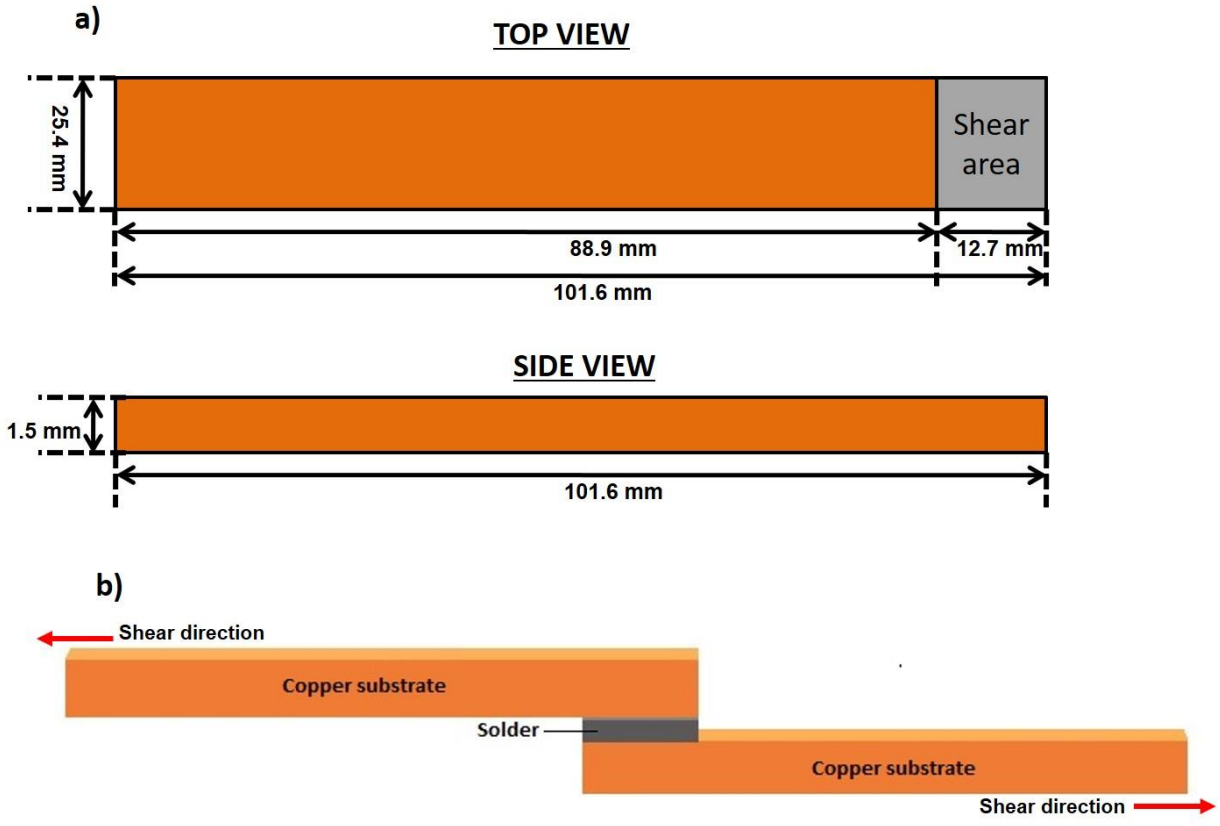

Figure 3 : a) Specifications of Cu-substrate (PCB FR4-Type), b) Schematic diagram of the single-lap shear test

3.0 Results and Discussions

3.1 Microstructure and phase analysis

Microstructure formations in the developed Sn-3.0Ag-0.5Cu (SAC305) composite solders were analyzed based on the post sintered and post reflowed samples. The sintered samples were etched and observed by using the Scanning electron microscope (SEM). Figure 4 depicts the micrograph of SEM for the post sintered pure SAC305 and KGC reinforced SAC305 composite solders with different weight percentage (wt.%) of kaolin geopolymer ceramic (KGC). It was observed the KGC particles as indicated as black particles are well distributed along the grain boundaries in the samples with addition of KGC in Figure 4 (b-e). The presence of distributed black particles indicates as KGC as proved by EDX analysis in Figure 5. The existence of Na, Al, Si, K, Ti and Fe by EDX corresponds to the elements in KGC systems. In addition, the reinforcement concentrations along the grain boundaries tend to hold the grains, hence prevent from grains dislocations and retard the growth of grains in the SAC305 solder matrix. Thus, the addition of KGC to the SAC305 solder matrix can improve the mechanical properties of solder.

In order to analyze the effect of KGC to the microstructures of SAC305 solder after reflow soldering process, cross-sectional image of pure SAC305 and KGC reinforced SAC305 composite solder were observed by using the scanning electron microscope, synchrotron micro-XRF and electron backscattered diffraction. Figure 6 shows the backscattered SEM image of post reflowed samples. Based on Figure 6, it confirmed there existed two different phases in each of the cross-sectioned samples. The two phases were primary β-Sn phase and eutectic phase. In the eutectic phase, primary intermetallic compound (IMC) of Cu_6Sn_5 and Ag_3Sn are dispersed in the eutectic area. The addition of KGC particles to the SAC305 lead-free solder greatly refined the β-Sn phase and reduced the size of primary Cu_6Sn_5 and Ag_3Sn as well. This therefore indicated that the addition of KGC particles into SAC305 lead-free solder contributes to the refinement effect in the microstructures of solder. Moreover, to precisely observe the microstructural changes in each of the samples, the area fraction of β-Sn phases and

eutectic phases were quantitively analyzed with the threshold image by using the J-image software as depicted in Figure 7. According to Figure 7,

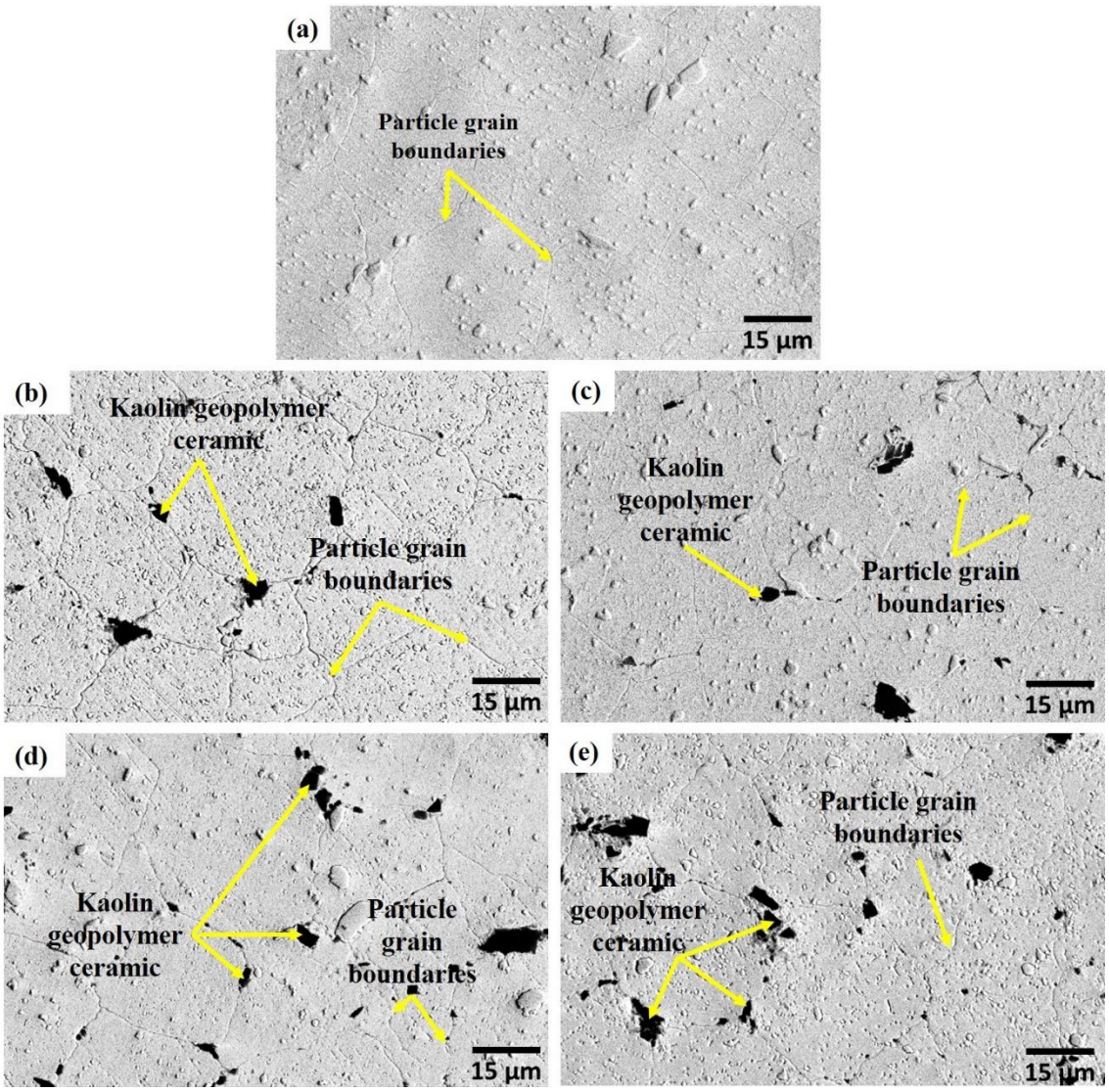

Figure 4: SEM micrograph of sintered SAC305/kaolin geopolymer ceramic samples showing distribution of KGC at a) 0 wt.% KGC, b) 0.5 wt.% KGC, c) 1.0 wt.% KGC, d) 1.5 wt.% KGC and e) 2.0 wt.% KGC

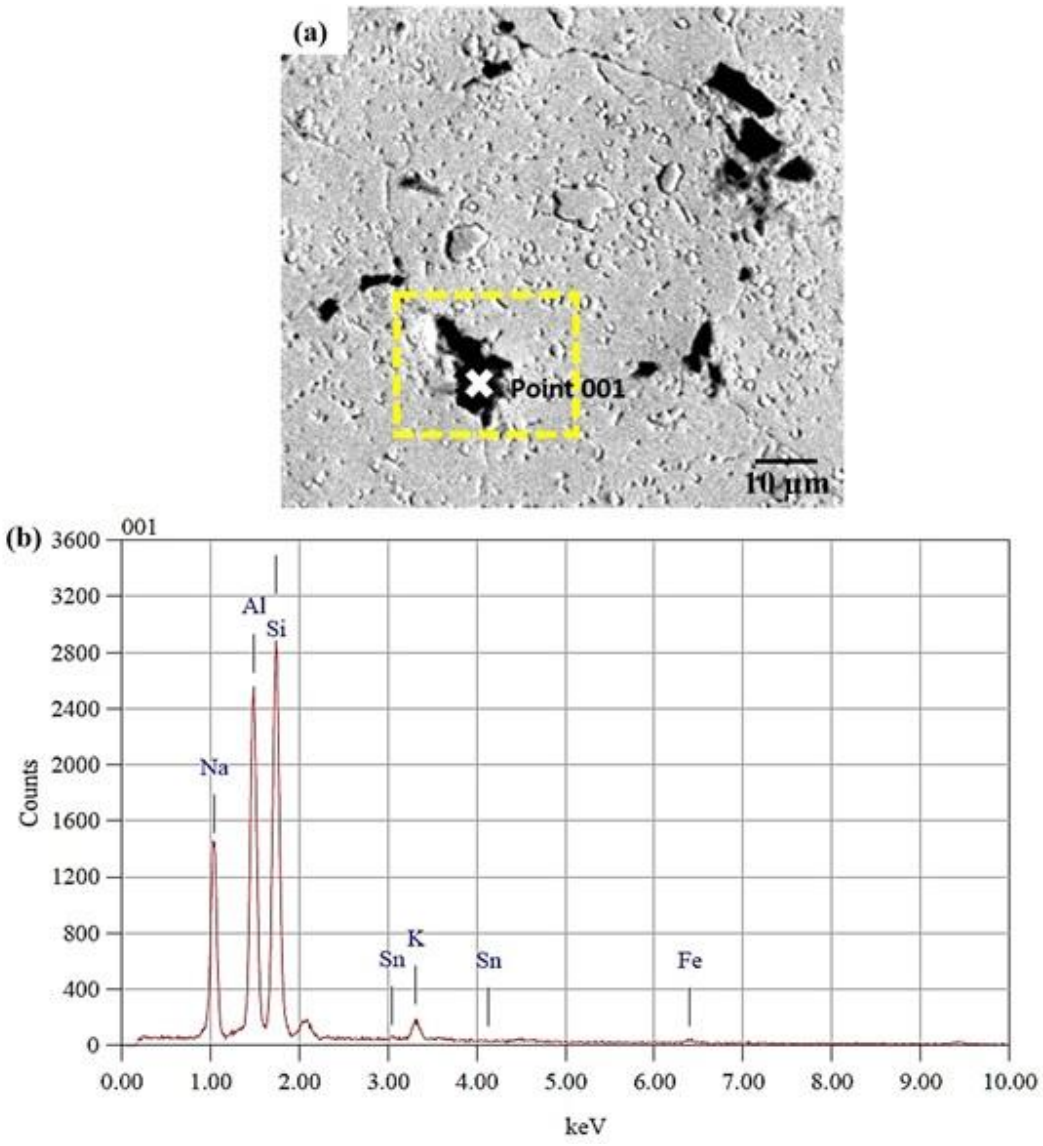

Figure 5 : a) SEM image of KGC reinforced SAC305 composite solder; b) Edx point analysis at point 001; c) Edx point analysis result of KGC reinforced SAC305 composite solder

additions of KGC particles influenced the area fraction of β-Sn and eutectic phases, in which the area fraction of β-Sn phases was slightly decreased with increased in the area fraction of eutectic phases (with smaller size of Cu_6Sn_5 and Ag_3Sn that dispersed in eutectic area) as the addition of KGC was up to 1.0 wt.%. However, as the amount of KGC added beyond 1.0 wt.% (in case of 1.5 wt.% and 2.0 wt.%), the area fraction of β-Sn phase increased with the decreased in the area fraction of eutectic phase. It was

noteworthy that, the addition of 1.0 wt.% KGC results in best refinement of microstructures in the SAC305 lead free solder.

The enhancement in the microstructure of SAC305 lead free solder is likelyattributed to the heterogeneous nucleation [9, 21, 36, 37]. During the reflow soldering, KGC particles finely dispersed throughout the molten solder matrix. According to the theory of heterogenous nucleation, the presence of KGC particles in an alloy of SAC305 solder matrix acted as heterogeneous nucleation sites for β-Sn and eutectic phases. The β-Sn and eutectic phases nucleate on the surface of KGC particles in the means to reduce the thermodynamic barrier of nucleation as suggested by Li et.al [14]. Hence, the nucleation rate was increased, reducing the size of the grains. Moreover, the higher nucleation rate of grains prevent from the grains ripening which consequently resulted with refined microstructures in SAC305 solder with addition of KGC particles. The similar phenomenon was also reported by Wang et. al [26], where addition of SiO_2 effectively serve as the grain refinement in solder alloys which may advantageously improve shear properties of composite solder alloys. As the best microstructure refinement was achieved with 1.0 wt.% KGC, the addition of KGC beyond this value slightly increases the area fraction β-Sn and decreases the area fraction of eutectic phase. This event might occur in the case of possible agglomeration of fine reinforcement particles in Sn solder matrix which may decrease the surface energy and consequently reduce the refining effect in the solder [9].

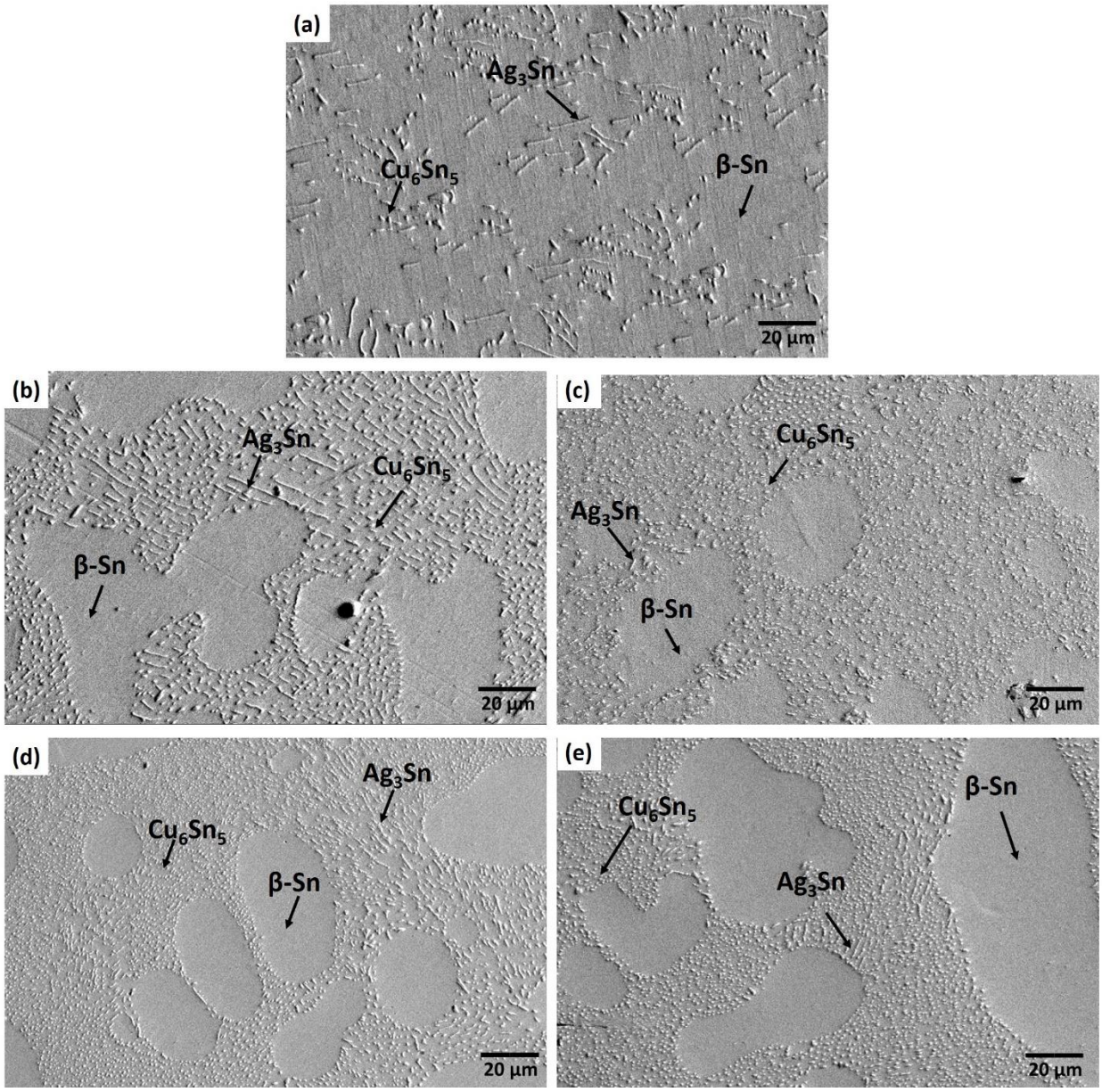

Figure 6: Microstructure of SAC305 with additions of a) 0 wt.%, b) 0.5 wt.%, c) 1.0 wt.%, d) 1.5 wt.% and e) 2.0 wt.% of KGC after reflowed on Cu substrate.

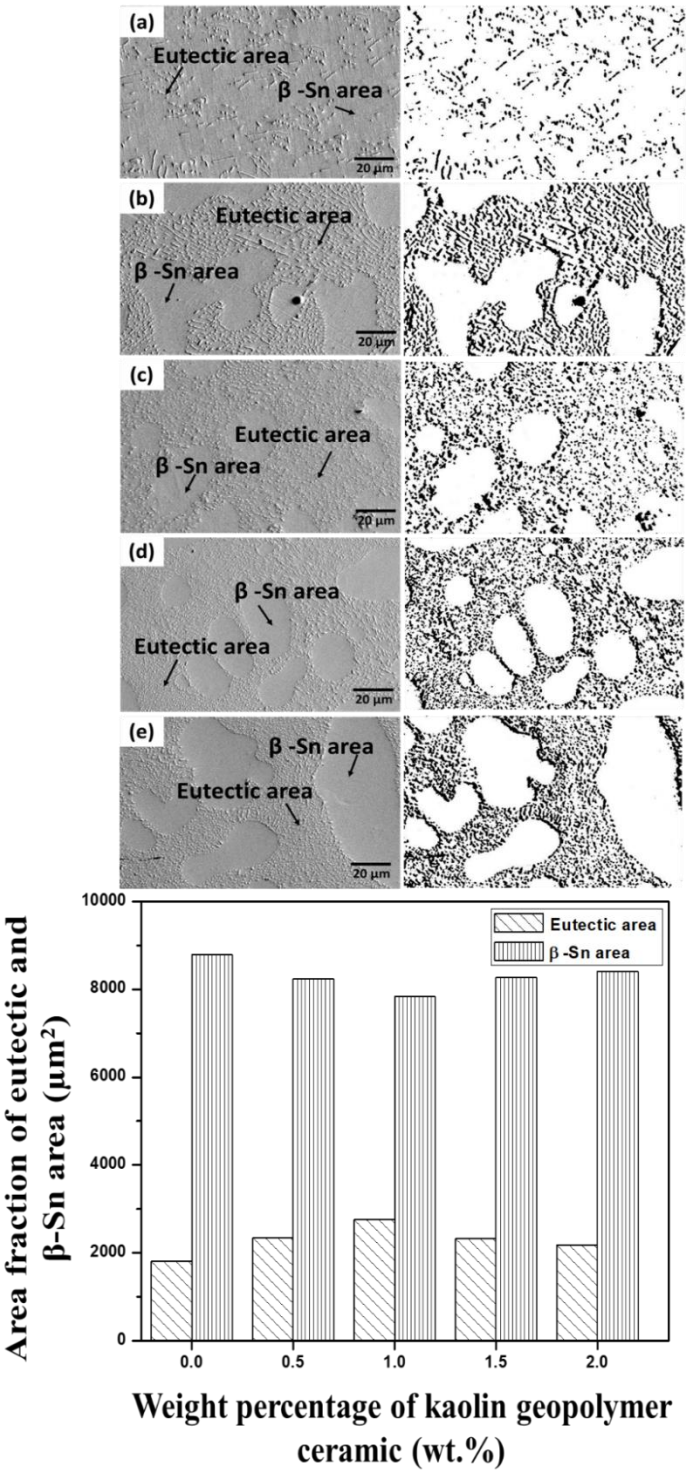

Figure 7 : Area fraction of β-Sn and eutectic phase of SAC305 lead free solder with different weight percentage (wt.%) addition of KGC ; a) 0 wt.% KGC, b) 0.5 wt.% KGC, c) 1.0 wt.% KGC, d) 1.5 wt.% KGC and e) 2.0 wt.% KGC, f)…

Intermetallic compound (IMC) layer forms from the reaction between molten solder and copper (Cu) substrate during soldering process [38]. The formation of IMC layer was vital in the solder joint since it indicates the existence of metallurgical bonding between the solder and substrate. Even so, the excessive formation of IMC layer is adverse to the solder joint reliability. In this research, IMC layer formed in the pure SAC305 solder and KGC reinforced SAC305 composite solder joints were analyzed based on the morphology and thickness of IMC layer. It was observed from Figure 8(a), the morphology of interfacial Cu_6Sn_5 layer consists of pointed and small scallop Cu_6Sn_5. However, as various weight percentage of KGC were added, the morphology of interfacial layer changed to the combination of shallow and small scallop. It is worth to observe that, there was no formation of pointed scallop in the KGC reinforced SAC305 composite solder. Since, the formation of the pointed scallop was undesired due to the pointed scallop will induce brittle fractures to the solder joint and contribute to crack initiation sites, as a result it adversely affects the performance of solder joints [9, 10]. The growth of pointed scallop at the interfacial layer caused by an increase in the concentration of copper atoms from substrate which diffused to the solder matrix and reacted with tin, resulting in growth of pointed scallop Cu_6Sn_5 as suggested by Li et. al [10].

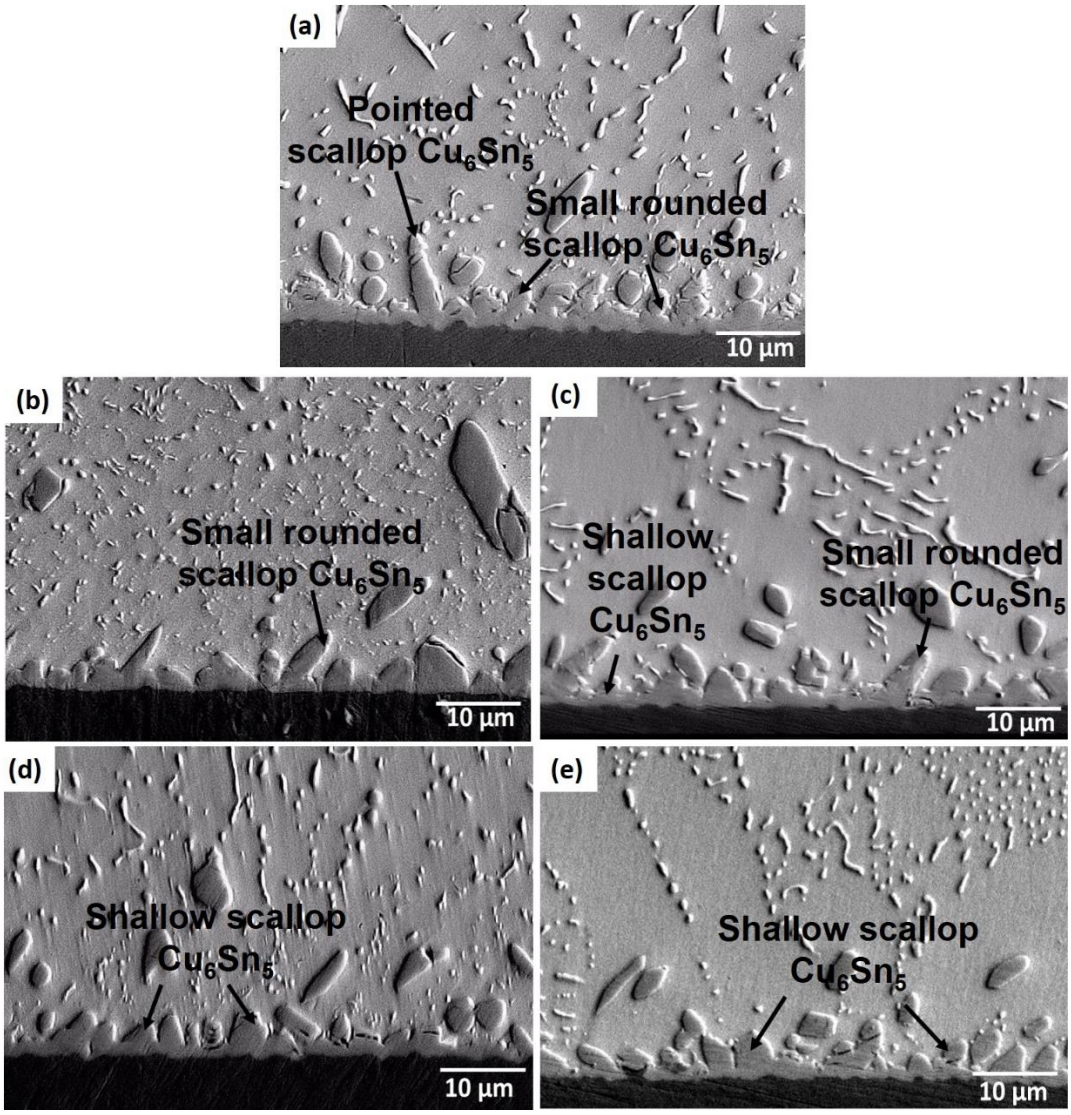

Figure 8 : Interfacial Cu_6Sn_5 IMC layer at different weight percentage of KGC ; a) 0 wt.% KGC, b) 0.5 wt.% KGC, c) 1.0 wt.% KGC, d) 1.5 wt.% KGC and e) 2.0 wt.% KGC

The average thickness of IMC layer for pure SAC305 solder and KGC reinforced SAC305 composite solder was measured and shown in Figure 9. Results proved that the thickness of IMC layer substantially decreased with the addition of KGC. The lowest average thickness of IMC layer was achieved with the addition of 1.0 wt.% KGC to the SAC305 solder. The reduction of 30% in average of IMC layer thickness was observed with the addition of 1.0 wt.% KGC in comparison to the pure SAC305 solder. However, the average thickness of IMC layer in the KGC reinforced SAC305 composite solder

slightly increased as the KGC added was beyond 1.0 wt.%. It is a worthwhile note that the reduction of the IMC layer thickness in the KGC reinforced SAC305 composite solder was ascribed to the effect of KGC added. The existence of KGC particles was proved by using the EDX line analysis along the interfacial layer as shown in Figure 10. The presence of Si and Fe elements by EDX analysis was owing to the KGC particles. Therefore, it can indicate that the presence of KGC along the interfacial IMC layer is able to suppress the growth of interfacial IMC during the soldering process.

The interfacial Cu_6Sn_5 IMC grains nucleated when the molten solder contacts with Cu substrate during the reflow soldering process and resulted in continuous IMC layer coverage at the Cu substrate/solder interface. As the concentration of Cu in SAC305 solder is less than 0.9 wt.%, the growth of scallop Cu_6Sn_5 IMC grains at the interface between substrate/solder required Cu atoms from the substrate to be dissolved simultaneously to the solder matrix [10]. In this case, the channels between the scallop Cu_6Sn_5 grains facilitates the growth of interfacial IMC in which it acts as the diffusion and dissolution paths for Cu atoms from the substrate to the solder matrix. Thus, the existence of KGC particles along the interfacial IMC layer as shown in Figure 10 acts as a barrier which reduces the diffusion of Cu from the substrate to the solder matrix and thus stabilizes the growth of interfacial IMC. As a result, thinner thickness of interfacial IMC is obtained in the KGC reinforced SAC305 composite solder than the pure SAC305 solder. Besides that, the suppression of the interfacial IMC was partly owing to the KGC reinforced SAC305 composite solder solidifies at lower undercooling than in pure SAC305 solder as demonstrated by DSC results in Table 2.

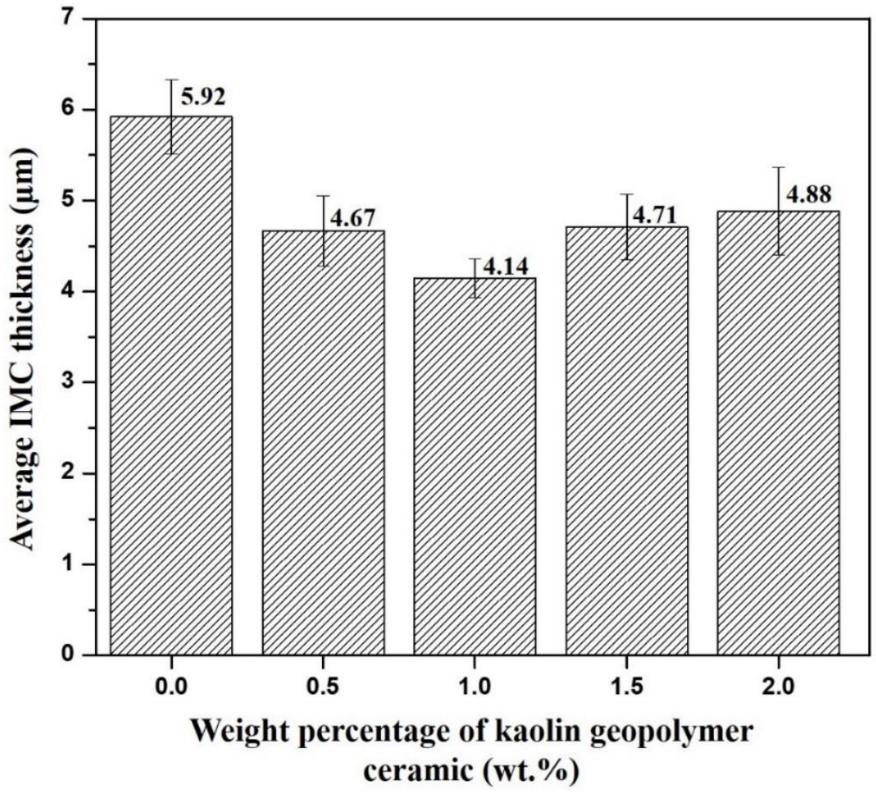

Figure 9: The influence of different weight percentage (wt.%) of KGC addition to the average IMC thickness of SAC solder joints.

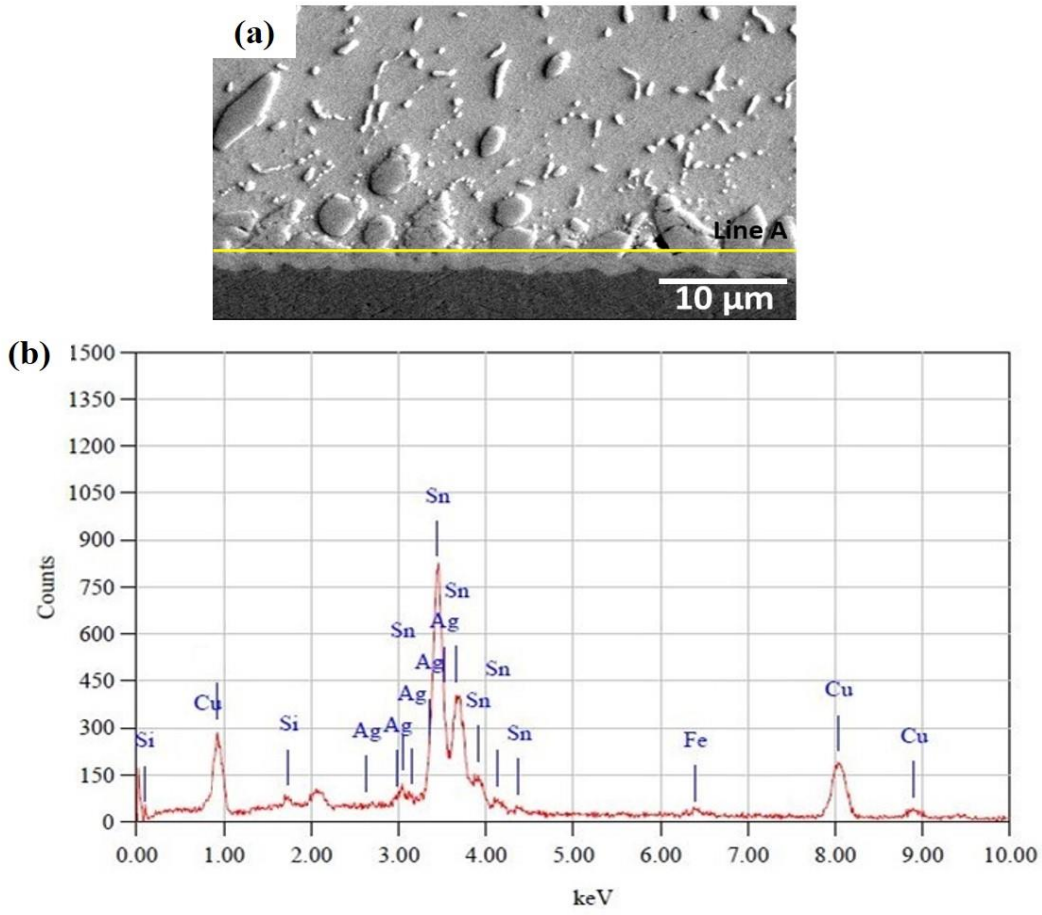

Figure 10 : a) Cross-sectional view of EDX line at interfacial IMC layer; b) EDX spectrum along the interfacial IMC layer

In order to determine the elemental distribution of Sn, Ag, Cu and other elements in KGC systems for as-reflowed samples, a higher precision elemental mapping analysis was carried out by using the synchrotron radiation source. Figure 11 shows the results obtained using the synchrotron micro-XRF from the pure SAC305 solder and KGC reinforced SAC305 composite solder. The higher intensity indicates the higher distributions for a specific element. FromFigure 11 (b) the elements of Al, Si, K, and Fe are clearly observed, which come from the KGC systems as proved by the X-ray fluorescence spectroscopy (XRF) in Table 1. These elements were dominantly distributed at the region of solder bulk area and only a little along the interfacial IMC of solder joint. The existence of these elements in the KGC reinforced SAC305 composite solder further

proved that, KGC particles can alter the microstructure formation, enhancing the properties of KGC reinforced SAC305 composite solder.

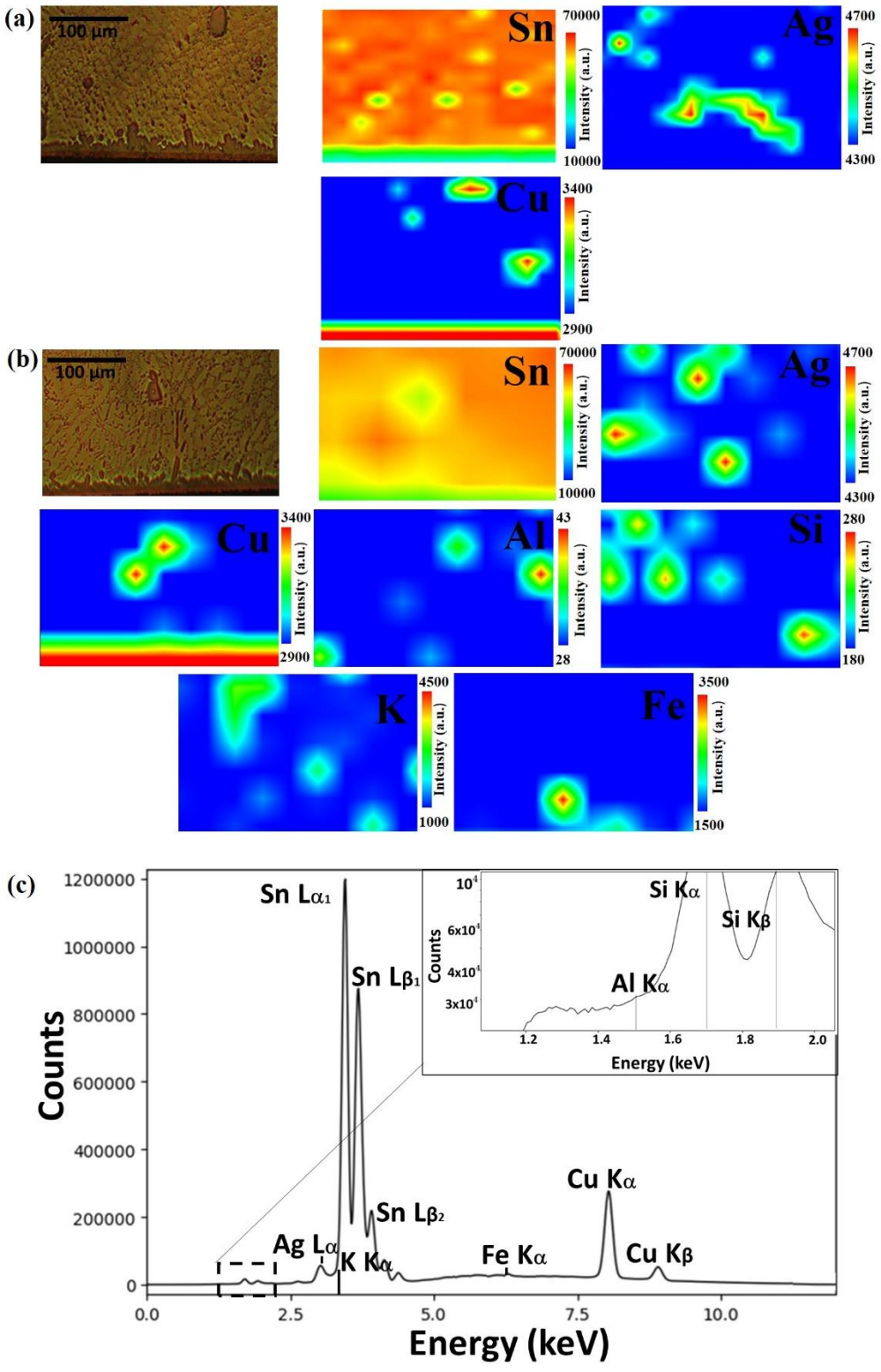

Figure 11 : The micro-XRF mapping area (a) Pure Sn-3.0Ag-0.5Cu (SAC305) (b)KGC reinforced SAC305 composite solder

Besides that, further details of microstructure were analyzed using EBSD. The orientation of crystal structure in the pure SAC305 and KGC reinforced SAC305 composite solder was investigated. The structure of beta-tin (β-Sn) is a body-centered tetragonal with lattice parameters of a = 5.632 nm, c = 0.3182 nm and c/a = 0.546 which possess anisotropic, thermal, mechanical and diffusion properties [39, 40]. Since Sn grains are the main matrix in the lead free solders, the orientation of the crystal structure may dictate the reliability of the solder joint. In this study, β-Sn grain structures and grain orientations are the subject of interest due to the structure of β-Sn may influence the mechanical response of solder joint under service conditions [41]. Figure 12 shows EBSD maps and inverse pole figures of the pure SAC305 and KGC reinforced SAC305 composite solder. The EBSD maps in Figure 12(b) and (d) shows that there are only single β-Sn crystal and no evidence of solidification twinning. By analyzing the inverse pole figure (IPF-y) in Figure 12(e) and (f), the crystal orientations for the β-Sn crystal are [110] and [010]. However, small addition of KGC particles to SAC305 slightly changes the orientation of β-Sn crystal to single orientation of [001] as depicted in Figure 12(f). Besides that, Figure 12(d) also shows the existence of KGC crystalline phases, and the major phase is nepheline. According to Yun Ming et.al [34], crystalline nepheline is the major phase existed in KGC for the heat-treated sodium based geopolymers.

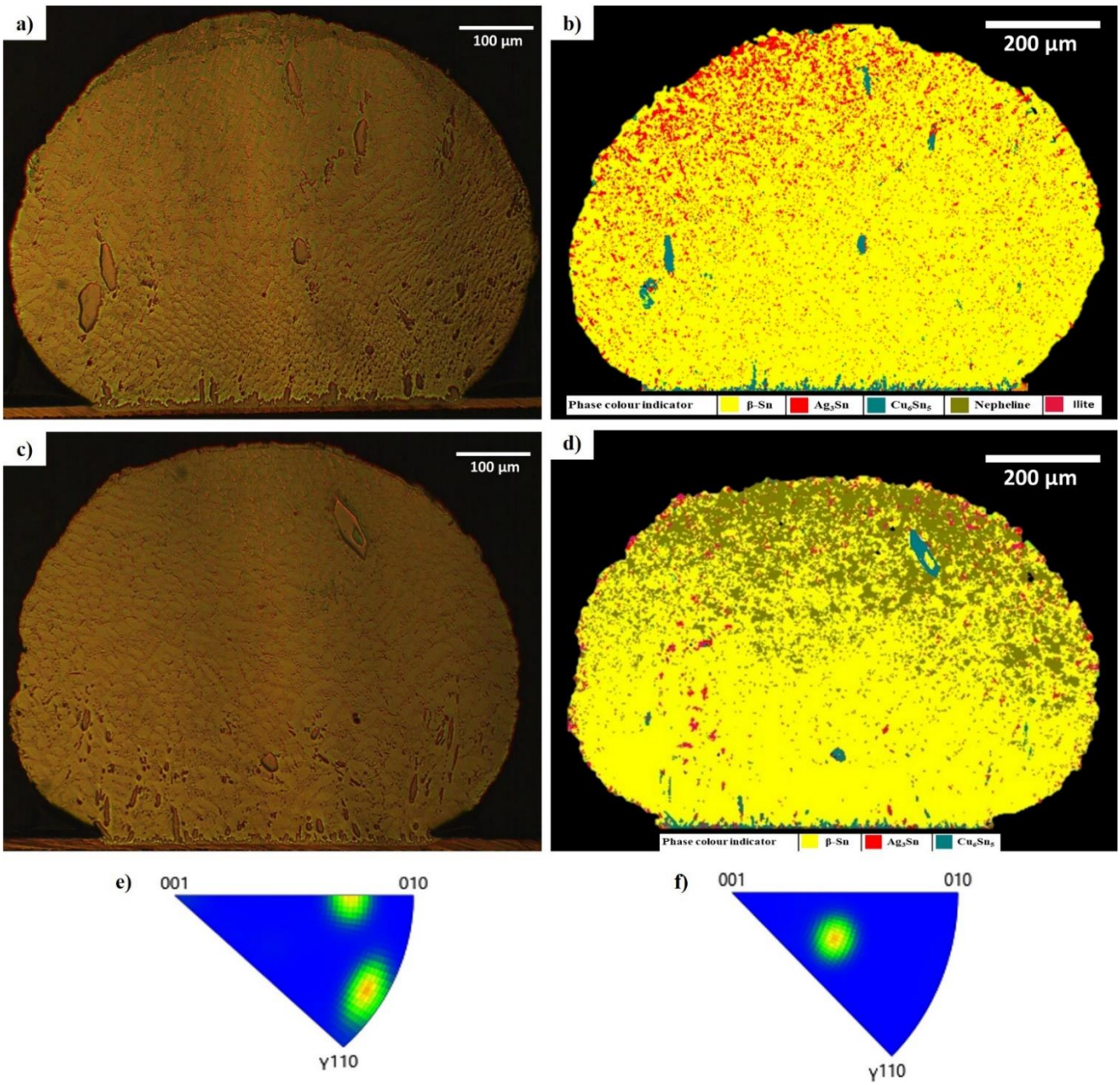

Figure 12 : OM and EBSD image of a) OM image of pure SAC305), b) EBSD maps of pure SAC305, c) OM image of KGC reinforced SAC305 composite solder, d) EBSD maps of KGC reinforced SAC305 composite solder, e) Inverse pole figure (IPF-y) of pure SAC305 and f) Inverse pole figure (IPF-y) of KGC reinforced SAC305 composite solder

Meanwhile, Figure 13 shows the strain contouring maps of pure SAC305 and SAC305 with the addition of KGC particles. In order to quantitively measure the strain contouring area in both samples, the area fraction of strain contours was measured as presented in Figure 13(c). By comparing the distribution of localized strain in both samples, pure SAC305 lead free solder has lower distribution of localized strain than the sample with the addition of KGC particles. The area fraction of localized strain measured in the pure SAC305 and KGC reinforced SAC305 composite solder are 36318 μm^2 and 72188 μm^2, respectively. In addition, it can also be seen the distribution of localized strain in the SAC305 with KGC additions is more homogenous than in the pure SAC305 lead free solder. In the pure SAC305, the localized strain may be due to the inhomogenous of Ag_3Sn and Cu_6Sn_5 intermetallics while in the KGC reinforced SAC305 composite solder is mainly well distributed by the KGC reinforcement.

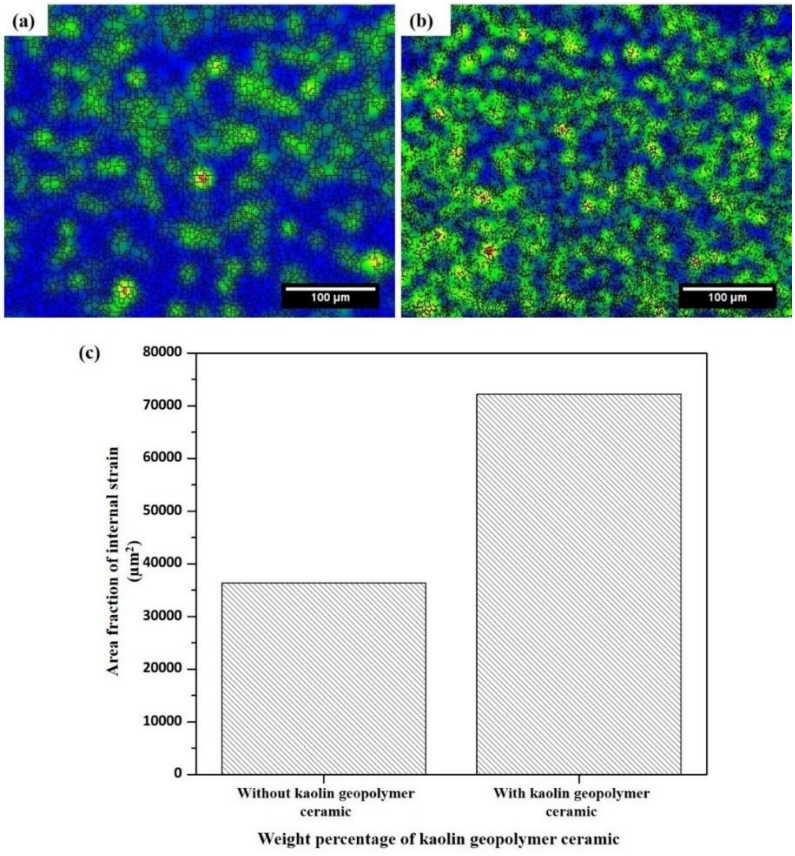

Figure 13 : Strain contour for (a) pure SAC305 and (b) KGC reinforced SAC305 composite solder (c) Area fraction of internal strain

In order to investigate the interactions between the bulk KGC and SAC305 lead free solder, synchrotron micro-XRF analysis was conducted. Figure 14 shows the results of micro-XRF elemental mapping conducted on samples of SAC/KGC. The samples for micro-XRF mapping consists of two parts: SAC305 lead free solder and KGC area as presents in Figure 14(a). The red colour regions indicate the highest concentration of the elements while blue colour regions indicate the lowest concentration of the elements in that particular area. According to the elemental mapping in Figure 14, it clearly shows that the elements, especially Al, Si and K from KGC systems migrated to the solder area part. In addition, point analysis was carried out at point 1 to confirm the presence of particular elements in the solder area part. Based on the spectrum at point 1, it was confirmed Al, Si and K elements from KGC systems existed in the solder area part. However, in this study the main concern was the migration of Al and Si elements since these elements were major elements in the geopolymer systems which formed the backbone of geopolymer chain, Si-O-Al and Si-O-Si bonds. The migration of some Al and Si elements to the solder area is believed due to the interactions of lead free solder elements and KGC elements as a bulk KGC was dipped in molten solder at 250 ºC. The heating process involved destabilized the KGC chains and thus promoted elements migration towards the solder area. Nevertheless, Na elements in KGC could act as alkali modifiers which may break the Si-O-Si and Si-O-Al bonding and thus lead to the migration of some elements to the solder area[42]. However, the data obtained for this experiment was not enough to justify and prove the migration mechanism and further detailed investigations need to be carried out.

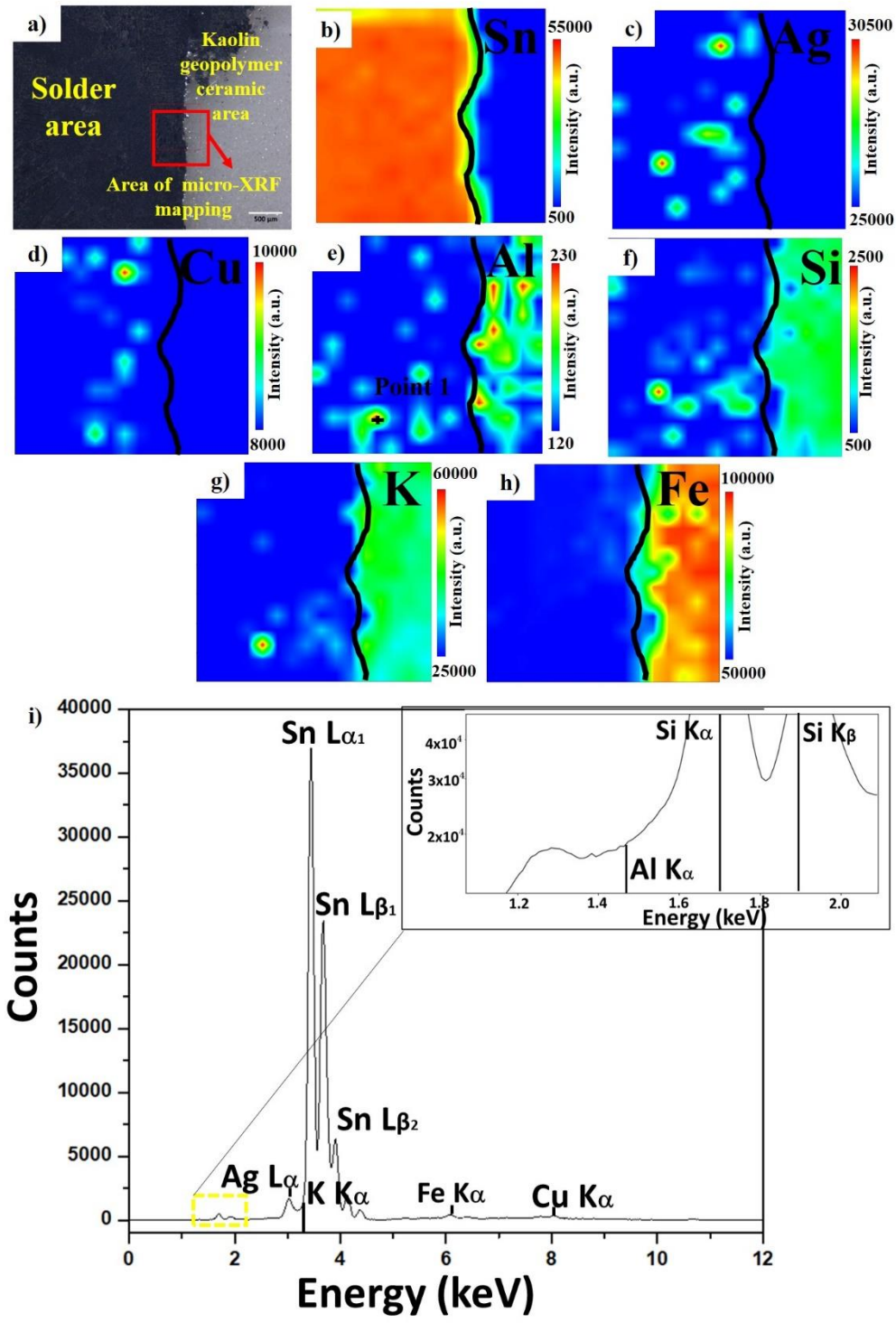

Figure 14 : Synchrotron Micro-XRF results: a) Image of synchrotron micro-XRF mapping area , b) Sn c) Ag d) Cu e) Al, f) Si g) K and h) Fe element mappings and i) point analysis spectrum at point 1

3.2 Spreadability

Solderability of solder can be evaluated through wettability and spreadability of solder on copper substrates subjected to reflow soldering. In general, solder alloys with higher spreading areas and lower contact angle are favored for reliable solder interconnections. In this study, wettability and spreadability of the pure SAC305 and composite SAC305 lead free solders were investigated by measuring the contact angle and spreading areas formed prior to reflow soldering process. In our previous study[add a reference here], we reported on the wettability of the pure SAC305 and composite SAC305 with the addition of kaolin geopolymer ceramic (KGC). The contact angle between the molten solder alloy and Cu substrates is related with the spreading areas, thus the evaluation on the spreadability of solder took placed. Figure 15 presents the spreadability of SAC305 with different addition of KGC on Cu substrates prior to reflow soldering process.

It was found that, the spreading areas increased firstly and then decreased with the increasing weight percentage (wt.%) of KGC particles. The spreading areas achieved maximum value of 91.45 mm^2 with the addition of 1.0 wt.% KGC, which is 19.1 % bigger than the pure SAC305 lead free solder. However, the spreading areas is degraded in SAC305 with the addition of KGC up to 2.0 wt.%, which is 80.40 mm^2. Therefore, from the results it is inferred that smaller wt.% addition of KGC contributes to the improvement in ability of solder having bigger spreading on Cu substrates. One reason for this could be due to the added KGC particles lower the interfacial surface energy and reduce surface tension as KGC particles accumulated at the interface between the flux and molten solder during the process of reflow soldering. In addition, as suggested by Chen at.al [25] and Sharma et.al [27], excess addition of the reinforcement in solders were able to increase the viscosity of solder and thus, obstructs the molten solder from further spreading. To conclude, unappropriated amount of reinforcements would deteriorate the solderability of solder alloys.

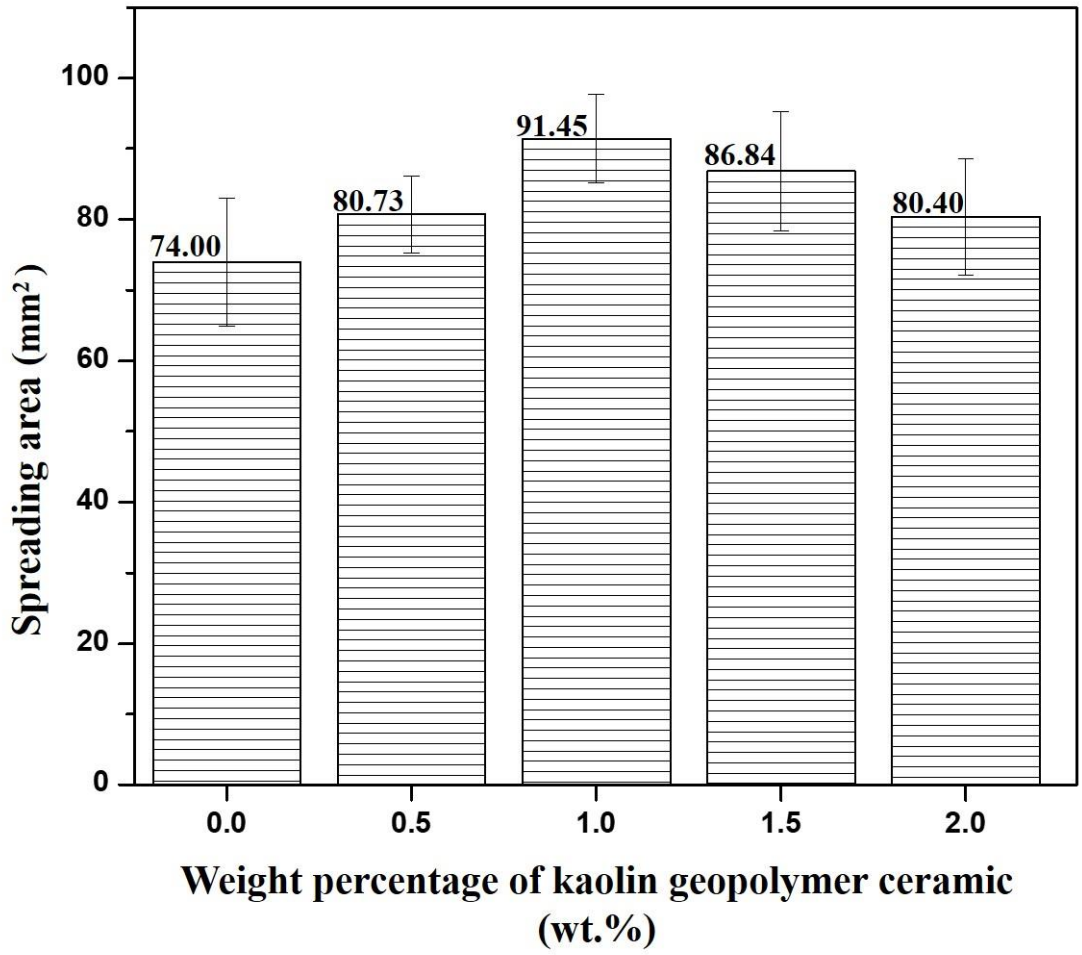

Figure 15 : Spreadability of SAC305 lead free solder with different weight percentage of KGC on copper substrate

3.3Thermal properties

Table 2 depicts the results obtained from DSC testing for the value of pasty range and melting temperature for the pure SAC305 and KGC reinforced SAC305 composite solders. These results show that, the addition of various amount of KGC could give little effect on the melting point of SAC305 lead free solder alloys. Hence the new composite solder system can be applied and integrated with the existing reflow profile during the soldering process without any adjustments needed. A slight increase in the melting point

of SAC305 lead free solder with addition of KGC was possibly due to the reinforcing particles may change the surface instability and variation in the physical properties of grain boundary/interfacial characteristics. Besides that, KGC particles reinforced in SAC305 lead free solder retard the solidification process where it acts as retardation sites for the solidification process of IMCs, as suggested by Fawzy et. al [43]. The results are in good agreement with the previous study reported by [43, 44].

Pasty range is an important thermal parameter in developing new composite solder alloys which can be measured by the difference between T_{endset} and T_{onset} during the heating process as presented in Table 2. In this study, the pasty range of pure SAC305 lead free solder was 8.92 °C. While, KGC reinforced SAC305 composite solder with different wt. % of KGC showed smaller pasty range temperature between 8.48 to 8.91 °C as compared to the pure SAC305 solder. Smaller pasty range can be inferred that, for the KGC reinforced SAC305 composite solder alloy there exists a partially liquid phase for a short time during the solidification process, in other words reducing the time of contact between the liquid phase and Cu substrates. Therefore, with smaller pasty range, the interfacial IMC in the reinforced KGC reinforced SAC305 composite solder alloy is thinner compared to the SAC305 lead free solder. On the other hand, large pasty range would give rise to fabrication issues such as porosity, hot tearing contraction during solidification and fillet lifting phenomena [45].

Thermodynamically, larger undercooling will result in a larger driving force for the IMCs to grow. Undercooling is defined as the difference between T_{onset} during heating and T_{onset} during cooling which is also related to the temperature range of solid phase nucleation in a liquid state until solidification [19]. The undercooling of the pure SAC305 and KGC reinforced SAC305 composite solders with different wt.% KGC is shown in Figure 16.Based on the result, the undercooling of the pure SAC305 lead free solder is 19.64 °C. While for KGC reinforced SAC305 composite solder, the undercooling is in the range between 14.89 to 16.81 °C. The lowest undercooling was achieved with the addition of 1.0 wt.% KGC. A significant decreased undercooling in the SAC305 with KGC addition was favorable. Moreover, the undercooling in solder alloy will influence the microstructure formation. The decrement in the undercooling of KGC reinforced SAC305

composite solder affects the microstructure formation as discussed at section 2.1 where the fraction of β-Sn phase decreased with smaller size of IMCs dispersed in eutectic area. The significant changes in the undercooling attributed to the effect of reinforcing particles. As suggested by El-Daly et.al [19], the decrement in the undercooling of SAC105 with addition of SiC is due to the decreased in the undercooling of β-Sn which inhibits the formation of IMCs. By inducing higher nucleation, the solidification of β-Sn will be faster which reduces the time for IMCs to grow, resulting in finer microstructures.

Table 2 : Pasty range and melting temperature from DSC testing of SAC305 and KGC reinforced SAC305 composite solder with different weight percentage of kaolin geopolymer ceramic

Solder	Pasty range (°C)	Melting temperature (°C)
SAC305	8.92	220.86
SAC305 + 0.5 wt.% KGC	8.52	220.55
SAC305 + 1.0 wt.% KGC	8.50	220.56
SAC305 + 1.5 wt.% KGC	8.48	221.01
SAC305 + 2.0 wt.% KGC	8.91	221.11

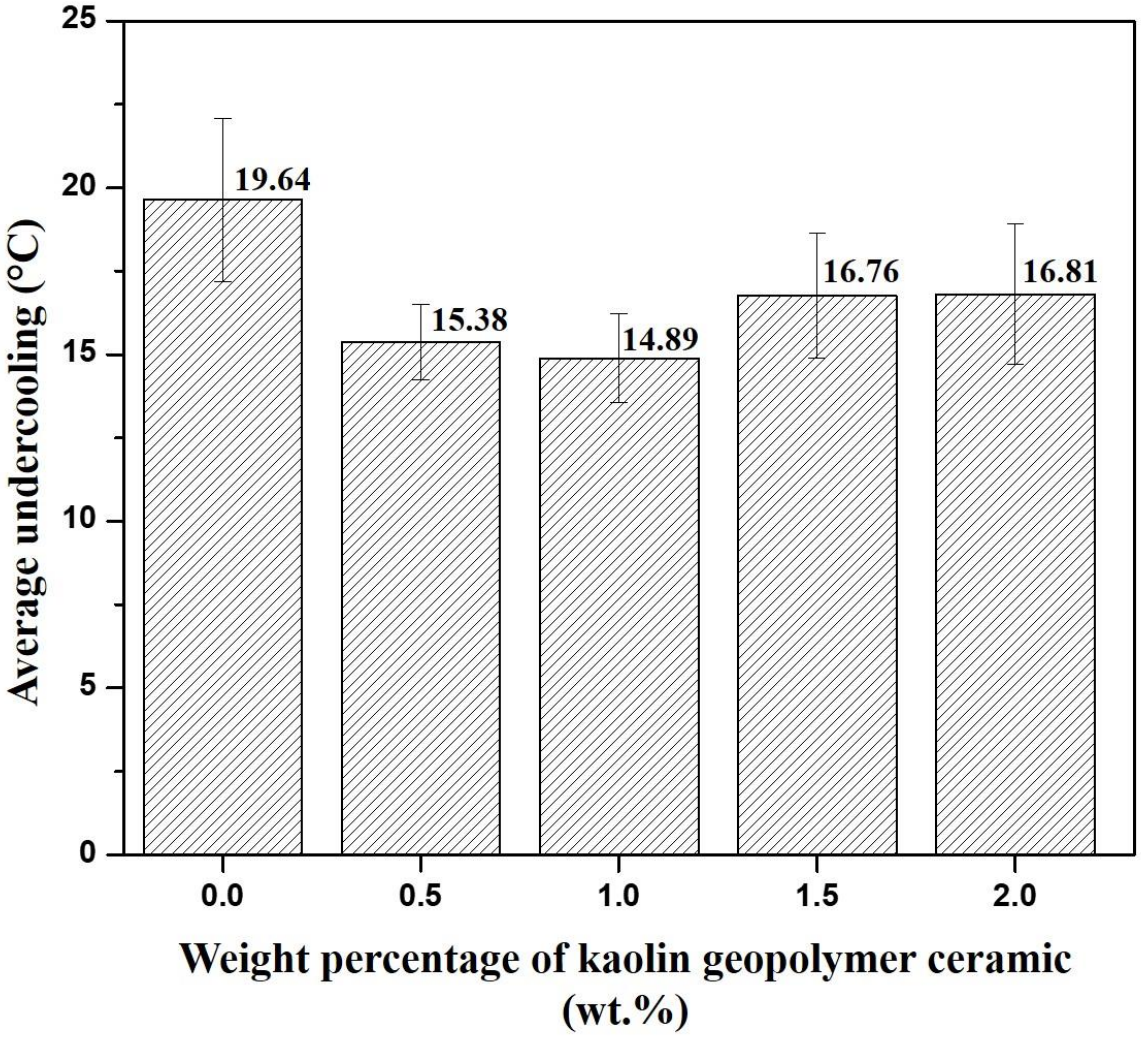

Figure 16 : The undercooling of pure SAC305 and KGG reinforced SAC305 composite solder with different weight percentage of KGC addition

3.4 Mechanical properties

Mechanical properties of the SAC305/x-KGC composite solder and monolithic SAC305 solder joints were determined based on the shear strength and failure behaviors. Figure 17 illustrates the average shear strength results of SAC305/x-KGC composite solder and SAC305 solder joints. It can be seen that, the addition of various wt.% of KGC positively influenced the shear strength of solder joints. The average shear strength of KGC reinforced SAC305 composite solder increased with the addition of various wt.%

KGC. Highest average shear strength was observed with the additions of 1 wt.% KGC with average 13.01 MPa compared to the non-added reinforcement solder with average 9.95 MPa. The increment of 31 % in the average shear strength was shown with additions of 1 wt.% KGC as compared to SAC305 solder joints. However, with the addition of KGC beyond 1 wt.% (1.5 wt.% and 2.0 wt.%), the average shear strength of solder joints slightly decreased from 13.01 MPa to 12.06 MPa and 10.32 MPa for 1.5 wt.% and 2.0 wt.% of KGC additions, respectively. Even so, the average shear strength of KGC reinforced SAC305 composite solders with KGC additions (1.5 wt.% and 2.0 wt.%) were still higher than SAC solder joints without the reinforcement.

In this study, the enhancement in the shear strength of KGC reinforced SAC305 composite solders is attributable to the theory of dispersion strengthening. Based on the theory, the existence of fine Ag_3Sn and Cu_6Sn_5 intermetallic particles which were well dispersed into the β-Sn matrix strengthens the composite solders. In addition, KGC particles that were uniformly distributed along the grain boundaries of the solder hinder the dislocation movement and impede the grain boundaries sliding. The phenomenon mentioned is known as pinning effects which explains the improvement in the shear strength of composite solders. Besides that, the improvement in the shear strength of composite solders can also be attributed to the controllable in the thickness of IMC layer formation at the interface between the composite solders and the Cu substrate as suggested by Wu et al. [46]. Thicker IMC layer is prone to brittle failure that will degrade the strength of the solder joint. In this study, the thickness of IMC layer in KGC reinforced SAC305 composite solders were proved to decrease with the additions of KGC reinforcement which partially improved the shear strength of the solder joints as compared to the pure SAC305 solder.

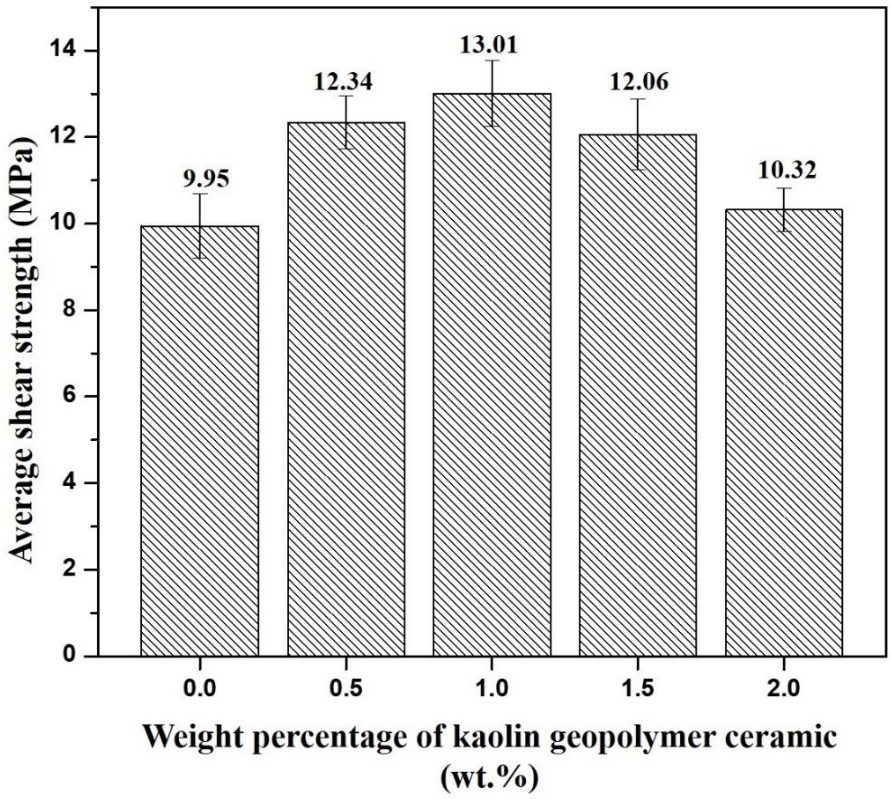

Figure 17: Average shear strength of different weight percentage of KGC addition to SAC305 lead free solder

In order to further understand the failure behaviors in KGC reinforced SAC305 composite solder and pure SAC305 solder, the post shear samples were observed. Figure 18 shows the fracture surface for the pure SAC305 and KGC reinforced SAC305 composite solders. Figure 18 (a) depicts the fracture behaviors of pure SAC305 solder. It was observed that the pure SAC305 solder exhibits brittle fractured mode with a smooth surface (little dimples). On the other hand, the fracture behaviors of KGC reinforced SAC305 composite solders showed a transformation in the mode of fracture, from brittle to ductile fracture mode with rough surface (indicated by circle shape). In addition, more dimples were observed in the samples containing KGC particles. The existence of more dimples correlates with the better plastic property for ductile materials. It is known that ductile materials normally experience large quantity of plastic deformations before failures along the loading directions. However, as the addition of KGC beyond 1.0 wt.%, large

dimples were observed at the fracture surface which explains the decrement in the shear strength of the samples. The formation of large dimples at the fracture surface is likely associated with the large brittle IMC as suggested by Z.H. Li et al. [9] and M.A.A Mohd Salleh et al. [21].

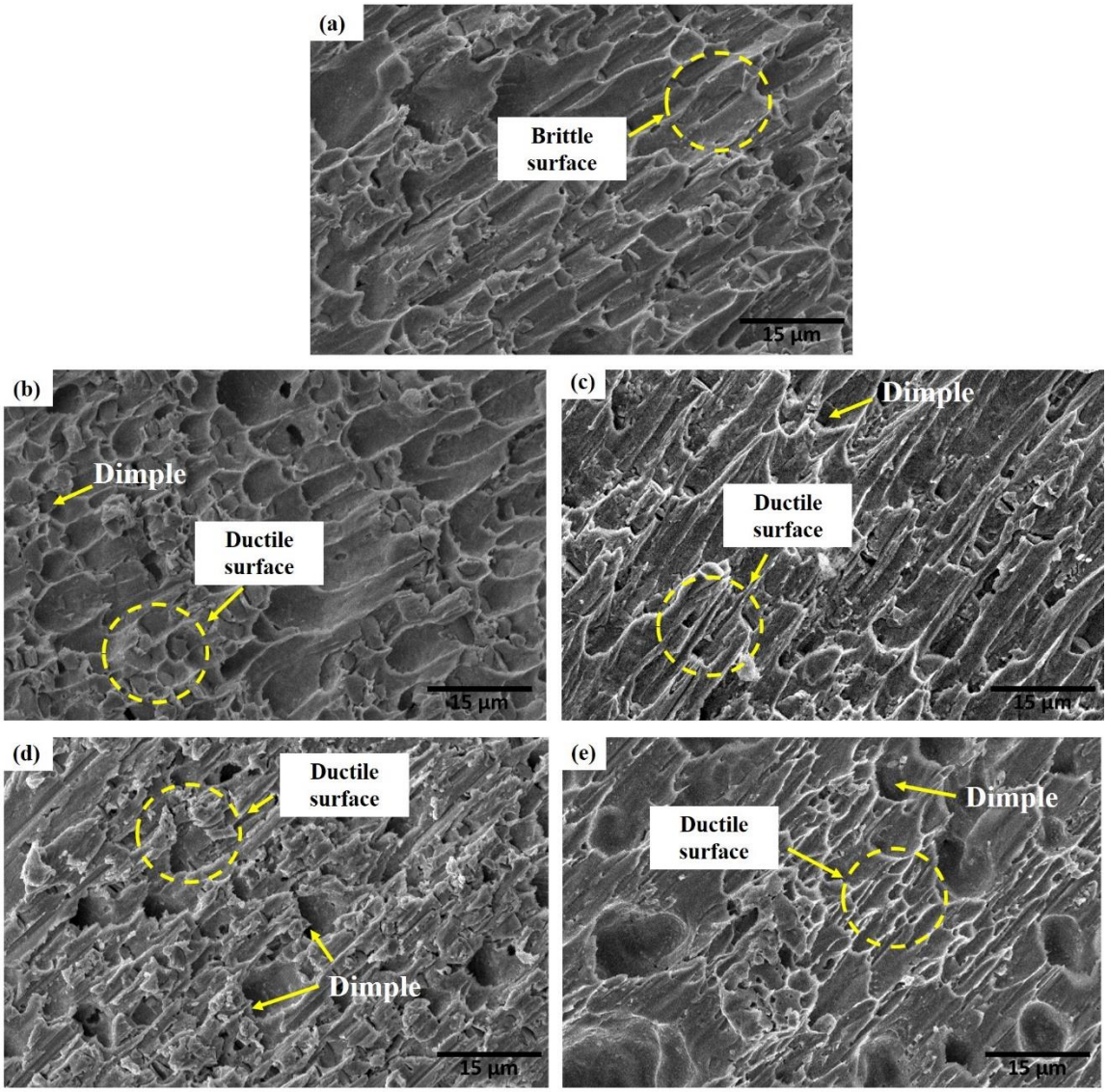

Figure 18: SEM micrograph of fracture surface of pure SAC305 and KGC reinforced SAC305 composite solder at different weight percentage of KGC; a) 0 wt. % KGC, b) 0.5 wt.% KGC, c) 1.0 wt.% KGC, d) 1.5 wt.% KGC and e) 2.0 wt.% KGC

4.0 Conclusions

The effects of kaolin geopolymer ceramic with various weight percentage to the Sn-3.0Ag-0.5Cu solder was elucidated in this paper. It can be concluded that;

(a) The addition of KGC alters the microstructure formation by decreasing the formation of β-Sn area and increasing the eutectic area with fine intermetallics of Cu_6Sn_5 and Ag_3Sn. KGC addition reduces the thickness of interfacial IMC with formation of small rounded scallop. The optimum thickness was found with an addition of 1.0 wt.% KGC. This was owing to the existence of KGC particles along the interfacial IMC acting as barrier that reduces the Cu diffusion from substrate to the SAC305 solder matrix and stabilizes the growth of interfacial IMC.

(b) The synchrotron micro- XRF confirmed that the distribution of KGC elements in the as-reflowed samples were majorly located at the solder bulk area. While EBSD testing shows that, the addition of KGC changes the orientation of β-Sn into single crystal orientation with high area of localized strain contouring. The interaction of SAC305 solder alloy with bulk KGC leads to the migration of elements Al and Si to the solder area part as Na elements in geopolymer system play a role as a bond breaker between Si-O-Si and Si-O-Al bonds.

(c) Improvement in the spreading area were achievd by the KGC addition, and the highest spreading area was achieved with the 1.0 wt.% KGC addition. The undercooling value was reduced significantly, and the lowest value of 14.89 °C was achieved with the 1.0 wt.% KGC addition. The reduction occurs due to that the KGC reinforcement plays a role in inducing higher nucleation and promoting faster solidification which results in finer microstructures.

(d) The average shear strength of the SAC305 lead free solder with 1.0 wt.% KGC has the highest strength of 13.01 MPa. The increment of 31% in average shear strength as compared to the pure SAC305 lead free solder proved the ability of KGC reinforcement in enhancing the mechanical properties of the composite SAC305 solder. In addition, the

small dimples with ductile failure mode were observed in the samples with 1.0 wt.% KGC addition.

Acknowledgements

This work was supported by Ministry of Higher Education, Malaysia under the fundamental research grant scheme (FRGS) (FRGS/1/2017/TK10/UNIMAP/03/2), Newton Fund Institutional Link Grant, ID 332397914, under the Newton-Ungku Omar Fund partnership. The grant is funded by the UK Department of Business, Energy and Industrial Strategy (BEIS) and Malaysia and delivered by the British Council.

References

1. Zaimi, N., et al., *The Effect of Geopolymer Ceramic Additions to The Wettability and Shear strength of Sn-Ag-Cu (SAC) Solder: A Preliminary Study.* IOP Conference Series: Materials Science and Engineering, 2019. **551**: p. 012081.
2. Mohd Salleh, M.A.A., et al., *Development of a microwave sintered TiO2 reinforced Sn–0.7wt%Cu–0.05wt%Ni alloy.* Materials & Design, 2015. **82**: p. 136-147.
3. Syahirah Mohamad Zaimi, N., et al., *The Effect of Geopolymer Ceramic Additions to The Wettability and Shear strength of Sn-Ag-Cu (SAC) Solder: A Preliminary Study.* IOP Conference Series: Materials Science and Engineering, 2019. **551**: p. 012081.
4. Zaimi, N.S.M., et al., *Influence of kaolin geopolymer ceramic additions to the wettability and electrical properties of Sn-3.0Ag-0.5Cu (SAC305) lead free solder.* IOP Conference Series: Materials Science and Engineering, 2019. **701**: p. 012033.
5. Liu, X.D., et al., *Effect of graphene nanosheets reinforcement on the performance of Sn · Ag · Cu lead-free solder.* Materials Science and Engineering: A, 2013. **562**(Supplement C): p. 25-32.
6. Jung, D.-H., A. Sharma, and J.-P. Jung, *Influence of dual ceramic nanomaterials on the solderability and interfacial reactions between lead-free Sn-Ag-Cu and a Cu conductor.* Journal of Alloys and Compounds, 2018. **743**: p. 300-313.
7. Coyle, R.J., K. Sweatman, and B. Arfaei, *Thermal Fatigue Evaluation of Pb-Free Solder Joints: Results, Lessons Learned, and Future Trends.* JOM, 2015. **67**(10): p. 2394-2415.
8. Ma, Z.L., et al., *Mechanisms of beta-Sn nucleation and microstructure evolution in Sn-Ag-Cu solders containing titanium.* Journal of Alloys and Compounds, 2018.
9. Li, Z.H., et al., *Effects of CeO2 nanoparticles addition on shear properties of low-silver Sn–0.3Ag–0.7Cu-xCeO2 solder alloys.* Journal of Alloys and Compounds, 2019. **789**: p. 150-162.
10. Li, Z.H., et al., *A diffusion model and growth kinetics of interfacial intermetallic compounds in Sn-0.3Ag-0.7Cu and Sn-0.3Ag-0.7Cu-0.5CeO2 solder joints.* Journal of Alloys and Compounds, 2019: p. 152893.
11. Gain, A.K., et al., *Microstructure, kinetic analysis and hardness of Sn–Ag–Cu–1wt% nano-ZrO2 composite solder on OSP-Cu pads.* Journal of Alloys and Compounds, 2011. **509**(7): p. 3319-3325.

12. Gain, A.K., Y.C. Chan, and W.K.C. Yung, *Effect of additions of ZrO2 nano-particles on the microstructure and shear strength of Sn–Ag–Cu solder on Au/Ni metallized Cu pads.* Microelectronics Reliability, 2011. **51**(12): p. 2306-2313.
13. Liu, Z., et al., *Effects of TiO2 nanoparticles addition on physical and soldering properties of Sn–xTiO2 composite solder.* Journal of Materials Science: Materials in Electronics, 2019. **30**(20): p. 18828-18837.
14. Li, Z.L., et al., *Effect of nano-TiO2 addition on microstructural evolution of small solder joints.* Journal of Materials Science: Materials in Electronics, 2016. **27**(6): p. 6076-6087.
15. Ramli, M.I.I., et al., *Effect of TiO2 additions on Sn-0.7Cu-0.05Ni lead-free composite solder.* Microelectronics Reliability, 2016. **65**: p. 255-264.
16. Tang, Y., G.Y. Li, and Y.C. Pan, *Effects of TiO2 nanoparticles addition on microstructure, microhardness and tensile properties of Sn–3.0Ag–0.5Cu–xTiO2 composite solder.* Materials & Design, 2014. **55**: p. 574-582.
17. Wen, Y., et al., *Reliability enhancement of Sn-1.0Ag-0.5Cu nano-composite solders by adding multiple sizes of TiO2 nanoparticles.* Journal of Alloys and Compounds, 2017. **696**: p. 799-807.
18. Mohd Salleh, M.A.A., et al., *Suppression of Cu6Sn5 in TiO2 reinforced solder joints after multiple reflow cycles.* Materials & Design, 2016. **108**: p. 418-428.
19. El-Daly, A.A., et al., *Novel SiC nanoparticles-containing Sn–1.0Ag–0.5Cu solder with good drop impact performance.* Materials Science and Engineering: A, 2013. **578**: p. 62-71.
20. El-Daly, A.A., et al., *Microstructural modifications and properties of SiC nanoparticles-reinforced Sn–3.0Ag–0.5Cu solder alloy.* Materials & Design (1980-2015), 2015. **65**: p. 1196-1204.
21. Mohd Salleh, M.A.A., et al., *Mechanical properties of Sn–0.7Cu/Si3N4 lead-free composite solder.* Materials Science and Engineering: A, 2012. **556**: p. 633-637.
22. M.A.A, M.S., et al., *Solderability of Sn-0.7Cu/Si3N4 lead-free composite solder on Cu-substrate.* Physics Procedia, 2011. **22**(Supplement C): p. 299-304.
23. Che Ani, F., et al., *The influence of Fe2O3 nano-reinforced SAC lead-free solder in the ultra-fine electronics assembly.* The International Journal of Advanced Manufacturing Technology, 2018. **96**(1): p. 717-733.
24. Fouzder, T., et al., *Influence of SrTiO3 nano-particles on the microstructure and shear strength of Sn–Ag–Cu solder on Au/Ni metallized Cu pads.* Journal of Alloys and Compounds, 2011. **509**(5): p. 1885-1892.
25. Chen, G., et al., *Performance of Sn–3.0Ag–0.5Cu composite solder with TiC reinforcement: Physical properties, solderability and microstructural evolution under isothermal ageing.* Journal of Alloys and Compounds, 2016. **685**: p. 680-689.
26. Wang, Y., et al., *Effects of nano-SiO2 particles addition on the microstructure, wettability, joint shear force and the interfacial IMC growth of Sn3.0Ag0.5Cu solder.* Journal of Materials Science: Materials in Electronics, 2015. **26**(12): p. 9387-9395.
27. Sharma, A., B.G. Baek, and J.P. Jung, *Influence of La2O3 nanoparticle additions on microstructure, wetting, and tensile characteristics of Sn–Ag–Cu alloy.* Materials & Design, 2015. **87**(Supplement C): p. 370-379.
28. Tsao, L.C., et al., *Effects of nano-Al2O3 particles on microstructure and mechanical properties of Sn3.5Ag0.5Cu composite solder ball grid array joints on Sn/Cu pads.* Materials & Design, 2013. **50**: p. 774-781.
29. Chuang, T.H., et al., *Strengthening mechanism of nano-Al2O3 particles reinforced Sn3.5Ag0.5Cu lead-free solder.* Journal of Materials Science: Materials in Electronics, 2011. **22**(8): p. 1021-1027.
30. Tsao, L.C., et al., *Effects of nano-Al2O3 additions on microstructure development and hardness of Sn3.5Ag0.5Cu solder.* Materials & Design, 2010. **31**(10): p. 4831-4835.

31. Dimas, D., I. Giannopoulou, and D. Panias, *Polymerization in sodium silicate solutions: A fundamental process in geopolymerization technology.* Journal of Materials Science, 2009. **44**: p. 3719-3730.
32. Jaya, N.A., et al., *Kaolin Geopolymer as Precursor to Ceramic Formation.* MATEC Web Conf., 2016. **78**: p. 01061.
33. Jaya, N.A., et al., *Characterization and Microstructure of Kaolin-Based Ceramic Using Geopolymerization.* Key Engineering Materials, 2016. **700**: p. 3-11.
34. Liew, Y.M., et al., *Formation of one-part-mixing geopolymers and geopolymer ceramics from geopolymer powder.* Construction and Building Materials, 2017. **156**: p. 9-18.
35. Jaya, N.a., M.M.A.B. Abdullah, and R. Ahmad, *Reviews on Clay Geopolymer Ceramic Using Powder Metallurgy Method*. Vol. 803. 2014. 81-87.
36. Tang, Y., G.Y. Li, and Y.C. Pan, *Influence of TiO2 nanoparticles on IMC growth in Sn–3.0Ag–0.5Cu–xTiO2 solder joints in reflow process.* Journal of Alloys and Compounds, 2013. **554**: p. 195-203.
37. Wang, X., et al., *Strengthening mechanism of SiC-particulate reinforced Sn–3.7Ag–0.9Zn lead-free solder.* Journal of Alloys and Compounds, 2009. **480**(2): p. 662-665.
38. Mohd Salleh, M.A.A., et al., *Rapid Cu6Sn5 growth at liquid Sn/solid Cu interfaces.* Scripta Materialia, 2015. **100**: p. 17-20.
39. Shen, Y.-A. and C. Chen, *Effect of Sn grain orientation on formation of Cu6Sn5 intermetallic compounds during electromigration.* Scripta Materialia, 2017. **128**: p. 6-9.
40. Chen, H., et al., *Grain Orientation Evolution and Deformation Behaviors in Pb-Free Solder Interconnects Under Mechanical Stresses.* Journal of Electronic Materials, 2011. **40**: p. 2445.
41. Lehman, L.P., et al., *Cyclic twin nucleation in tin-based solder alloys.* Acta Materialia, 2010. **58**(10): p. 3546-3556.
42. Jabraoui, H., et al., *Effect of Sodium Oxide Modifier on Structural and Elastic Properties of Silicate Glass.* The Journal of Physical Chemistry B, 2016. **120**.
43. Fawzy, A., et al., *Effect of ZnO nanoparticles addition on thermal, microstructure and tensile properties of Sn–3.5 Ag–0.5 Cu (SAC355) solder alloy.* 2013. **24**.
44. Tsao, L.C., *An investigation of microstructure and mechanical properties of novel Sn3.5Ag0.5Cu–XTiO2 composite solders as functions of alloy composition and cooling rate.* Materials Science and Engineering: A, 2011. **529**(Supplement C): p. 41-48.
45. Eid, E.A., A.M. Deghady, and A.N. Fouda, *Enhanced microstructural, thermal and tensile characteristics of heat treated Sn-5.0Sb-0.3Cu (SSC-503) Pb-free solder alloy under high pressure.* Materials Science and Engineering: A, 2019. **743**: p. 726-732.
46. Wu, N., S. Ismathullakhan, and Y. Chan, *Effect of 1 wt% ZnO nanoparticles addition on the microstructure, IMC development, and mechanical properties of high Bi content Sn–57.6Bi–0.4Ag solder on Ni metalized Cu pads.* Journal of Materials Science: Materials in Electronics, 2014. **25**: p. 2169-2176.